Cluster radioactivity half-lives

M. Ivascu

Central Institute of Physics, Bucharest

I. Silisteanu

Joint Institute for Nuclear Research, Dubna

Fiz. Elem. Chastits At. Yadra **21**, 1405–1455 (November–December 1990)

Phenomenological and microscopic approaches to the description of the lifetimes of heavy nuclei with respect to spontaneous cluster decay are reviewed. Some simplified models are considered, and a multichannel microscopic model is described in detail. Questions related to the decay mechanism and the influence of nuclear structure and also the mechanism of excitation of the fragments are discussed. An attempt is made to obtain spectroscopic information on the basis of general microscopic–macroscopic schemes of analysis. The main attention is devoted to study of the coupling between intermediate structures and collective resonances of the compound nucleus. A comparison with experimental data is made, and important properties of cluster decays are discussed in detail.

INTRODUCTION

The investigation of spontaneous nuclear decays is one of the most important branches of nuclear physics. In recent years, interesting results have been obtained in it, and they have significantly extended our traditional picture of α decay and the mechanism of spontaneous fission. It is sufficient to note that the outcome of recent extensive theoretical and experimental investigations in this direction was the discovery of an entirely new form of spontaneous decay of heavy nuclei intermediate between α decay and spontaneous fission and involving the emission of heavy fragments and the formation of residual nuclei close to the doubly magic nucleus ^{208}Pb. This new phenomenon received various names in the literature: magic radioactivity, complex radioactivity, cluster decay, etc., each of which reflects, when taken together, the diversity and generality of the process.

The first theoretical predictions[1] and experimental observations of spontaneous cluster decay[2] stimulated much interest and further investigations of the process.

Since cluster decay is intermediate as regards mass and charge between α decay and spontaneous fission, it is not surprising that all lifetime calculations were made in the framework of one of these schemes, and the mechanism of the process was based formally on either α decay or spontaneous fission.

Now, after exceptionally laborious investigations, mainly semiquantitative and purely phenomenological, advances have been achieved in the formation of a unified picture of these three forms of spontaneous decay: α decay, cluster decay, and spontaneous fission. It appears that the main part is played by the "valley" structure of the barrier, which contains complete information about the different decay modes. To describe the lifetimes in this picture, it is exceptionally important to have information about the potential energy and the kinetic energy (mass parameters).

The potential energy can be described by a fairly simple parametrization as a sum of a smooth part (given by the liquid-drop model) and a relatively small shell correction. The description of the mass parameters is much more difficult, owing to their complex dependence on the internal structure of the system, the nuclear deformation, pairing effects, quantum effects, collective coordinates, etc. In addition, the continuous variation of the mass parameters (as the system evolves) leads to a change in the potential energy, and this has a strong influence on the lifetime. Therefore, it is a difficult task to obtain reliable information about the lifetimes from analysis of the potential energy and the mass parameters. But it is precisely such an analysis that makes it possible to obtain a direct indication of the main properties of spontaneous decays: low statistical probability, exponential law, passage through an intermediate state with energy much greater than the energies of the initial states of the nucleus and the final states of the fragments, and the effects of coupling of the intermediate structures to resonances, which are observed in the reverse reactions with complex fragments.

The main part of this review is devoted to a presentation of the practical schemes used to calculate the lifetimes. The various phenomenological and microscopic approaches, and also the connections between them, are presented in a very compact and general form in this paper. As a consequence, we can, in the framework of a unified mathematical formalism, not only obtain already known important results (of course, by means of sensible and widely accepted approximations) but also construct new approximation schemes and methods of studying spontaneous cluster decay.

This paper is based on the results obtained and published by the authors since 1980.

In Secs. 1 and 2 we discuss the main properties of the spontaneous decays—α decay, spontaneous fission, and cluster decay—and the problem of the penetrability of one-dimensional and multidimensional barriers in these processes. Section 3 is largely devoted to an analysis of phenomenological approaches to the description of cluster decay.

Section 4 is devoted to the microscopic description of cluster decay. The attempt to understand the part played by resonance scattering in cluster decay led us at once to the problem of the collective resonances of an unstable system formed by the fusion of (identical) fragments. With a view to studying and obtaining microscopic information about cluster decay, we make a microscopic–macroscopic analysis of modern experimental data. In this section we devote particular attention to studying the effects of nuclear deformation on the lifetimes of spontaneous cluster decay.

 0090-4759/90/060599-24$04.00

In the final section, we give the main conclusions of our paper.

1. INFORMATION ABOUT SPONTANEOUS CLUSTER DECAY

First hypotheses

The first conjecture of the existence of cluster decay in the region of heavy nuclei was advanced in 1924. Considering data on the anomalously high abundance of free nitrogen in uranium ores, the Englishman Foot[28] advanced the conjecture of nitrogen radioactivity of uranium.

In 1966, Shukolyukov[29] made a similar conjecture in order to explain the observed excess of neon and argon isotopes in uranium minerals. Moreover, he suggested that uranium nuclei fission asymmetrically with the emission of light neon and argon isotopes.

Finally, we mention that excesses of ^{86}Kr isotopes in meteorites of various types were explained by Alexander[30] as the result of asymmetric fission of nuclei with $A \simeq 300$, which also leads to the production of isotopes in the region of ^{208}Pb.

At the present time, there are no proofs of a connection between these geological or astronomical observations and the phenomenon of spontaneous cluster decay.

Theoretical predictions

Theoretical studies in which a new form of spontaneous radioactivity was predicted appeared before the experimental observations. In the studies of Ref. 1, general ideas about nuclear stability led to a first discussion of the possible existence of a new decay phenomenon, cluster decay, intermediate between α decay and fission. Cluster decay was interpreted as extremely asymmetric two-body fission. The first estimates of cluster-decay lifetimes were made by Sandulescu, Poenaru, and Greiner. They showed that some cluster decays could occur with probabilities that could be directly measured. The actual recommendations (Ref. 1, Fig. 7) proved to be correct only in certain cases (emission of ^{24}Ne and ^{28}Mg nuclei from Th and U isotopes). Analysis of cluster decay in the first Gamow model[1] showed that the greatest probability must be associated with a decay leading to the formation of magic (or semimagic) fragments ($A_1 = 208$, $Z_1 = 82$, $N_1 = 126$, $A_2 = 14$, 24, 28, $Z_2 = 6$, 8, 10, 12, 14, $N_2 = 8$, 20).

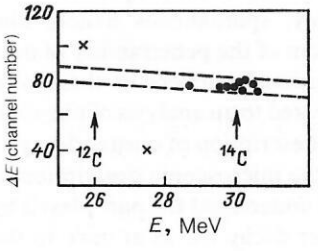

FIG. 1. Two-dimensional ΔE–E spectrum obtained by Rose and Jones[2] for emission of a ^{14}C cluster from the ^{223}Ra nucleus. The points represent events corresponding to emission of the ^{14}C cluster; the broken lines show the region that bounds the possible ^{14}C events (the results of calibration); the lower cross corresponds to a fourfold superposition of α-particle pulses, and the upper cross to an event observed during the time of the experiment.

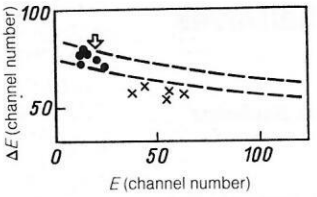

FIG. 2. Two-dimensional ΔE–E spectrum obtained by Aleksandrov *et al.*[3] in measurements with the ^{223}Ra nucleus. The points are events corresponding to emission of ^{14}C nuclei; the broken curves are the results of the calibration. The region of events of fourfold superpositions of α-particle pulses is bounded by the continuous curves, while the region of fivefold superpositions is shown by the crosses.

It is important to note that the first elementary theory of cluster decay[1] did not fully deny the possibility of the phenomenon because the penetrabilities were artificially overestimated by several orders of magnitude.

Discovery of ^{14}C decay

In 1984, Rose and Jones[2] made a first observation of spontaneous emission of ^{14}C nuclei from ^{223}Ra. When this discovery was reported, the group of Aleksandrov *et al.*[3] performed an experiment to look for ^{14}C emission for ^{223}Ra. Thus, the investigation of Ref. 3 was an independent confirmation of the discovery of a new form of spontaneous emission of ^{14}C from ^{223}Ra. The decisive factor in the discovery of cluster decay was the choice of the decaying nucleus. The choice was due to the gain in the decay energy for nearly magic nuclei, as a result of which we have the greatest penetrability (i.e., the greatest decay probability).

The particles emitted from the source were identified by the ΔE–E method. This method made it possible to detect ^{14}C events on the huge background of α particles. Figures 1 and 2 show the ΔE–E spectra of ^{14}C events observed in Refs. 2 and 3.

The result of Ref. 2 was confirmed later by other groups (Figs. 3–5)[4,6] by means of the ΔE–E method[4,5] and track detectors.[6]

The results of all these studies are given in Table I. Rose and Jones[2] calculated the penetrability (in the simple Gamow model) for $^{12-15}$C, ^{15}N, ^{18,19}O, and ^{28}Mg emission from the nuclei ^{227}Th, ^{227}Ac, ^{223}Ra, ^{219}Rh (^{235}U series) and on the basis of the Gamow factors concluded that they had most probably observed emission of ^{14}C from ^{223}Ra in their experiments.

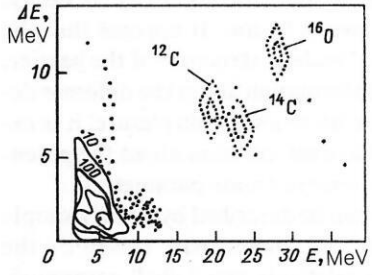

FIG. 3. The ΔE–E spectrum for emission of a ^{14}C cluster from the ^{223}Ra nucleus, obtained by the group of Gales *et al.*[4] The dotted lines are the results of the calibration; the points are the results of detection of a ^{14}C event from the ^{223}Ra nucleus.

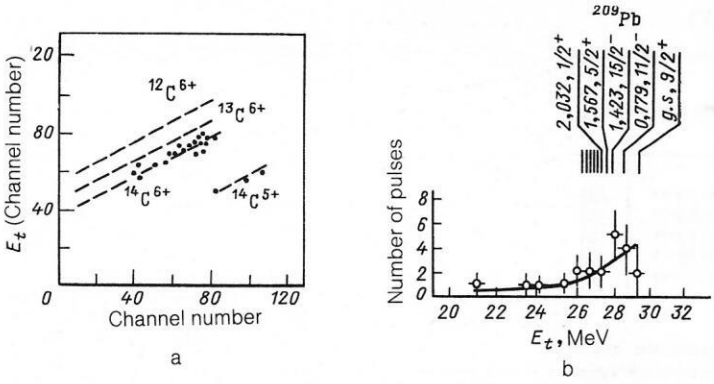

FIG. 4. The ΔE–E spectrum in measurements with the ^{223}Ra nucleus, obtained by the group of Kutschera *et al.*[5] (a) (the points are detected ^{14}C events; the broken lines are the results of the calibration) and the events in (a) represented as a function of the total energy E_t (b). The upper part of the figure shows the ground and excited states of ^{209}Pb.

We mention that such a theoretical analysis to establish the greatest penetrability of the Coulomb barrier was proposed earlier in Ref. 1.

The observation of the first spontaneous radioactive decay of ^{14}C from ^{223}Ra gave a tremendous impetus to new experimental and theoretical investigations.

The spontaneous emission of ^{14}C nuclei was soon confirmed for a number of other nuclei, namely, ^{221}Fr and ^{221}Ra (Refs. 6 and 7), ^{222}Ra (Refs. 6 and 8), ^{224}Ra (Ref. 6), ^{225}Ac (Ref. 7), and ^{226}Ra (Refs. 7 and 8) (see Figs. 3–5 and Table I).

In their turn, the theoreticians could renormalize their model parameters by using this rich collection of experimental data. The new theoretical predictions[21–25] were much more accurate and indicated that the cluster decay with greatest energy must be realized with appreciable probability, leading to the production of magic (or semimagic) fragments.

Discovery of Ne, Mg, and Si decays

All these decays were investigated at Dubna and Berkeley by means of track detectors. Observation of ^{24}Ne decay was made for ^{230}Th (Ref. 9), ^{231}Pa (Ref. 10), ^{232}U (Ref. 11), ^{233}U (Refs. 12 and 13), and ^{234}U (Refs. 14, 15, and 16).

Observation of ^{28}Mg decay was made for ^{234}U (Refs. 14, 15, and 16) and ^{238}Pu (Ref. 17), and of ^{30}Mg for ^{237}Np (Ref. 9).

Finally, ^{32}Si decay was recently observed for ^{238}Pu (Ref. 17), for which $B \approx 10^{-16}$, and ^{34}Si decay was observed for ^{241}Am (Refs. 9 and 18). All these results were discussed in detail in Price's review.[20]

The discovery of the spontaneous emission of C, Ne, Mg, and Si nuclei made it possible to examine more deeply the problem of the decay of heavy nuclei. In addition, the new discoveries are a stimulus for the construction of a general deductive theory capable of describing the various decays in a unified manner.

It has now become clear that spontaneous cluster decay is a general phenomenon and that the world of unstable nuclear systems has been shown to be much richer than we knew hitherto.

2. GENERALIZATION OF GAMOW'S THEORY

Decay energy

We begin by considering the influence of the main factors on the rate of spontaneous radioactive decays. One of these factors is the decay energy. Using only the binding energy, one can conclude that there is a basic possibility of emission by nuclei of protons and strongly bound fragments such as He, C, O, ..., etc. In connection with the fact that the mean binding per nucleon is particularly large for medium and some light nuclei (He, C, O, ...), many heavy nuclei are energetically unstable with respect to decay into two nuclei, $A = A_1 + A_2$, and the decay energy

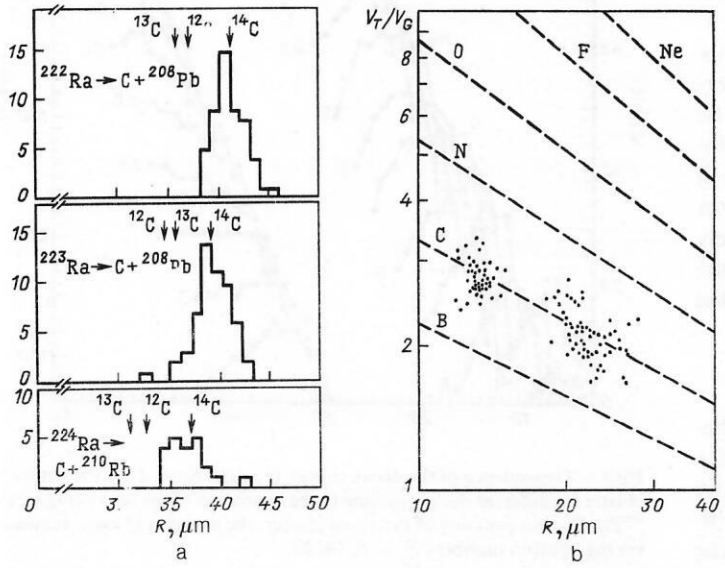

FIG. 5. The results of the experiments of Price *et al.*[6] on observation of ^{14}C emission from the nuclei ^{222,223,224}Ra: a) ratio of the measured and calculated (from the energy Q) residual radii R; b) dependence of the selectivity of the manifestation of V_T/V_G on the residual radius R. The points represent the results of observations along the ^{14}C trajectory; the broken lines show the results of the calibration.

TABLE I. Experimental data on ^{14}C emission from ^{223}Ra ($Q = 31.8$ MeV).

Source intensity, μCi	Exposure time, days	Method* of observation	Calibration	Number of events	$\lg T_c$	$B = T_\alpha/T_c$ **	Ref.
3,3	184	a	—	19	15,06±0,15	$(8,5\pm2,5)\cdot10^{-10}$	[2]
85	30	a	^{12}C, ^{14}N	7	15,11±0,22	$(7,6\pm3,0)\cdot10^{-10}$	[3]
210	5	b	^{14}C	11	15,25±0,2	$(5,5\pm2,0)\cdot10^{-10}$	[4]
9,2	6	c	$^{12-14}$C, N, O	24	15,32±0,14	$(4,7\pm1,3)\cdot10^{-10}$	[5]
See Ref. 6	See Ref. 6	d	$^{12, 13, 14}$C	56	15,20±0,07	$(6,1\pm1,0)\cdot10^{-10}$	[6]

*a) ΔE–E telescope and Si detector; b) magnetic spectrometer, ΔE–E telescope, and Si detector; c) magnetic spectrometer, ΔE–E telescope, and gas detector; d) track (plastic) detectors.
**$T_\alpha = 9.85\times10^5$ sec.

$$Q = E - E_1 - E_2 \qquad (1)$$

is positive for many different (A_1, A_2) combinations.

A strong influence on the decay energy is exerted by closed shells, which are boundary lines between regions of stable and unstable nuclei. It can be seen from Fig. 6 that the energy of cluster decay has clear peaks, which are associated with the closing of neutron shells (and subshells of the light fragment with $N_2 = 8, 14, 20$).

We shall see later that the structure of the initial and final nuclei puts a rather strong imprint on the decay energy and, therefore, on the decay probability. We encounter similar circumstances in the case of α decay and fission and in deep inelastic transfer reactions.[31]

Decay barriers

Despite the energy instability, many decays are not realized for a variety of reasons, but above all (we shall see this later) because of the extremely low penetrability of the Coulomb barrier. The penetrability reaches a significant value in some extreme cases: proton and two-proton decays[32] ($A > 6$ and $Z > N$) and α decay ($A > 100$), for which the emitted charge is small, and for cluster decay into fragments intermediate in charge and mass between α particles and fission fragments.

The height of each barrier can be estimated approximately as the energy of the electrostatic repulsion of the fragments when they touch, and this energy is always greater than the decay energy.

One may ask why different spontaneous decays are observed in a precisely defined zone of masses, and what determines the decay intensity. Answers to these questions can be obtained from a discussion that to a certain degree is analogous to those made in Refs. 1, 26, and 27 in consideration of the processes of α decay, spontaneous fission, and cluster decay. It is obvious that any decay into two positively charged fragments is difficult by virtue of the existence of the Coulomb barrier, and spontaneous decays can be regarded as processes of below-barrier tunneling.

Equations of motion

Below-barrier tunneling is a quantum-mechanical phenomenon. Investigation of tunneling processes in complex nuclear systems and, especially, in cluster decay is currently one of the most topical problems of theory and experiment.

From the theoretical point of view, a solution of the Schrödinger equation with approximate boundary conditions contains complete information about the tunneling process.

Many problems of quantum-mechanical tunneling can be studied on the basis of one- and multidimensional models for the potential barriers. In most of these models, the dynamical behavior of the unstable nucleus is described by means of a Hamiltonian that depends on certain independent collective coordinates $q_1, \ldots, q_N$:

$$H = H_1 + H_2 + T(q_1, \ldots, q_N) + V(q_1, \ldots, q_N), \qquad (2)$$

where H_1 and H_2 are the internal Hamiltonians of the fragments, T is the kinetic-energy operator corresponding to the classical kinetic energy T_{cl},

$$T = -\frac{1}{2}\hbar^2 \sum_{i,\,j=1}^{N} \frac{1}{D}\frac{\partial}{\partial q_i} M_{ij} D \frac{\partial}{\partial q_j}, \quad D = \det M_{ij}; \qquad (3)$$

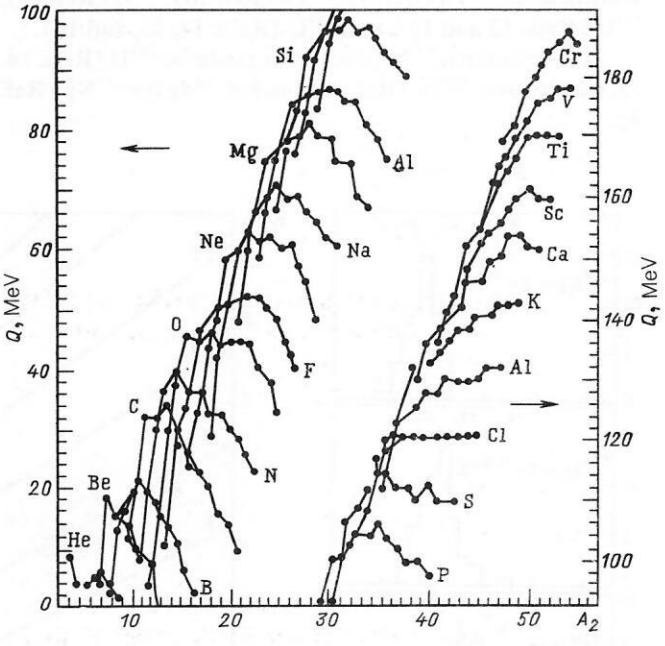

FIG. 6. Dependence of the decay energy Q on the mass A_2 of the emitted cluster for different decays leading to the formation of the heavy fragment ^{208}Pb. For the emission of the given cluster, the energies Q have maxima for the neutron numbers $N_2 = 8, 14, 20$.

$$T_{\text{cl}} = \frac{1}{2} \sum_{i,\, j=1} M_{ij} \dot{q}_i \dot{q}_j, \tag{4}$$

and M_{ij} are the mass parameters. To study the evolution of an unstable system consisting of A_1 and A_2 nucleons, it is necessary to investigate the interaction of the two clusters A_1 and A_2.

The wave function of such a system can be represented in the form

$$\psi = \hat{\mathcal{A}} \{\Phi_1 (A_1)\, \Phi_2 (A_2)\, U (q_1, \ldots, q_N)\}. \tag{5}$$

If the intrinsic cluster functions Φ_1 and Φ_2 are fixed, then the function U of the relative motion depends only on the choice of the interaction. To obtain equations of motion for U, it is necessary to substitute (5) in the many-particle Schrödinger equation

$$(H - E)\, \psi = 0, \tag{6}$$

and the function U can be found by solving a differential or integro-differential equation.

In the one-dimensional case, the classical and quantum-mechanical Hamiltonians have the form

$$H_{\text{cl}} = H_1 + H_2 + \frac{1}{2} M (q)\, \dot{q}_1^2 + V (q); \tag{7}$$

$$H = H_1 + H_2 - \frac{1}{2} \hbar^2 \frac{1}{[M (q)]^{1/2}} \frac{d}{dq} \frac{1}{[M (q)]^{1/2}} \frac{d}{dq} + V (q). \tag{8}$$

In the one-dimensional models, one usually employs an "effective" potential, which is a sum of the nuclear, Coulomb, and centrifugal potentials of the two fragments ($q \equiv r$ is the distance between the centers of mass of the fragments):

$$V (r) = V_{\text{Coul}} (r) + V_{\text{nuc}} (r) + V_{\text{cent}} (r). \tag{9}$$

The Schrödinger equation for the degree of freedom r has the form

$$\left[-\frac{1}{2} \hbar^2 \frac{1}{(M (r))^{1/2}} \frac{d}{dr} \frac{1}{(M (r))^{1/2}} \frac{d}{dr} + V (r) - Q \right] U (r) = 0, \tag{10}$$

where $Q = E - E_1 - E_2$.

The transformation[33]

$$x (r) = \int_0^r [M (r)/M_0]^{1/2}\, dr, \tag{11}$$

where M_0 is an arbitrary constant mass, transforms Eq. (10) into an ordinary Schrödinger equation with constant mass:

$$\left[-\frac{\hbar^2}{2M_0} \frac{d^2}{dx^2} + \overline{V} (x) - Q \right] \overline{U} (x) = 0, \tag{12}$$

where

$$\left.\begin{aligned} \overline{V} (x) &= \overline{V} (x (q)) = V (q); \\ \overline{U} (x) &= \overline{U} (x (q)) = U (q). \end{aligned}\right\} \tag{13}$$

Thus, the variation of the mass as a function of the dynamical variable q leads to a variation of the potential. In the general case, $\overline{V}(x)$ has a complicated form, and it is very difficult to solve the equation. In some special cases, for a potential well and for an inverted oscillator, $\overline{V}(x)$ and $\overline{U}(x)$ can be obtained in analytic form.[33,34,48]

Probability of barrier penetration

To determine the probability P of tunneling penetration through the barrier in the general case, it is necessary to solve (10) with the boundary condition of an outgoing wave as $r \to \infty$. If a specific functional form is given for $M(r)$, then our problem is greatly simplified.

In the case $M(r) = M_0$, semiclassical solutions are satisfactory everywhere except in the region near the classical turning point; there are formulas that ensure matching of the solutions obtained for the interior and exterior parts of the barrier. In this case[26,35]

$$P = [1 + \exp S]^{-1} \approx \exp (-S), \tag{14}$$

where

$$S = \frac{2}{\hbar} \int_{r_1}^{r_2} [2M_0 (V (r) - Q)]^{1/2}\, dr \tag{15}$$

is the action integral; $M_0 = A_1 A_2/(A_1 + A_2)$; r_1 and r_2 are the turning points: $V(r_1) = V(r_2) = Q$.

We shall discuss the general case $M(r) \neq \text{const}$ in detail in Sec. 3. Of course, the one-dimensional description of the barrier penetrability is a simplification, but it is a comparatively good approximation for studying α decay, cluster decay, and spontaneous fission.

It should be mentioned that the first predictions of cluster decay[1] were based on elementary calculations in accordance with Eq. (14), in which the potential $V(r)$ (9) was determined from scattering reactions.

To determine the penetrability in multidimensional models, it is more advantageous to use the approach proposed earlier for the study of spontaneous fission.[36] We mention here only the main result of this approach. In the collective adiabatic description of the fission process, the probability P of barrier penetration is usually calculated in the semiclassical approximation:

$$P = [1 + \exp S (L_{\min})]^{-1} \approx \exp (S (L_{\min})), \tag{16}$$

where

$$S (L) = \frac{2}{\hbar} \int_{L_1}^{L_2} \{2M (L) [V (L) - Q]\}^{1/2}\, dL \tag{17}$$

is the action integral calculated along the path $L = \{q_1, \ldots, q_N\}$ defined in the space of deformations q_i; $M(L)$ is the "effective" mass parameter along the trajectory L; Q is the decay energy.

The effective mass parameter in (17) is

$$M (L) \equiv M_{LL} (L) = \sum_{i,\, j} M_{q_i q_j} \frac{dq_i}{dL} \frac{dq_j}{dL}, \tag{18}$$

where $M_{q_i q_j}$ are the components corresponding to the deformation parameters q_i and q_j.

In Refs. 1 and 54, a study was made of the penetrability of a two-dimensional (r, η) barrier, and it was shown that the influence of the orthogonal degree of freedom reduces mainly to a change of the barrier height and an enhancement of cluster decay. We mention that concrete results for cluster decay on the basis of the expressions (16) have not yet been obtained. In Sec. 3, we discuss in detail the problem of the penetrability of two-dimensional barriers.

Decay rate λ

If the decay occurs under normal conditions as a result of a number of independent events (this is assumed in Gamow's theory)—formation of a cluster, collision with the barrier, and quantum-mechanical tunneling—we must multiply all the probabilities in order to obtain the total probability (or rate) of the decay:

$$\lambda = nFP = \frac{\ln 2}{T}, \tag{19}$$

where n is the number of collisions with the barrier in 1 sec, F is the cluster-formation factor, and P is the barrier penetrability. It is obvious that for independent events Eq. (19) is invalid. We mention here that the equation of motion (10) was obtained on the basis of one strong assumption, the matrix elements of the Hamiltonian between the bound states and the continuum states being ignored. Inclusion of these elements leads to the appearance of the formation amplitude as an inhomogeneity of Eq. (10).[37] Of course, this shows that P depends on F, and Eq. (19) is invalid.

Finally, we point out that the simplicity of Eq. (19) is matched by the difficulty of the problem of determining the spatial dependence of the individual probabilities and the spatial separation of these events.

Study of spontaneous nuclear decays in α decay and fission leads to the conclusion that the decisive factor in these processes with extremely low decay rates λ_α and λ_f is the barrier penetrability. The same conclusions were reached in Ref. 1 for cluster decay, in which the barrier penetrability P remains the principal factor, the first estimates showing that $\lambda_f \lesssim \lambda_c$.

The lifetimes of radioactive nuclei exceed the characteristic nuclear time (10^{-22} sec) by several tens of orders of magnitude (see Figs. 16 and 18). As we have already shown, there are two main factors that ensure these immense lifetimes. First, barrier effects can lead to long lifetimes relative to the emission of charged particles or clusters. Second, allowance for quantum and structure effects also leads to a very low probability of statistical decay.

The delay time due to high barriers can be estimated in the quantum-mechanical one-dimensional model:

$$\Delta t = \int_{-\infty}^{\infty} dx\, [|\psi(x)|^2 - |\psi_0(x)|^2]. \tag{20}$$

where ψ_0 is the solution of the homogeneous equation (6) [with $V(x) = 0$]. In the semiclassical approach, the energy E can be regarded as a function of ψ. Then from (6)

$$(H-E)\frac{\partial\psi}{\partial E} - \psi = 0; \tag{21}$$

$$\psi^*\psi = \frac{\hbar^2}{2M_0}\frac{\partial}{\partial x}\left[\psi^*\frac{\partial\psi}{\partial E} - \frac{\partial\psi}{\partial E}\frac{\partial\psi}{\partial x}\right]; \tag{22}$$

$$\int_{-x}^{x}\psi^*\psi\, dx = -\frac{\hbar^2}{2M_0}\left[\psi^*\frac{\partial^2\psi}{\partial x\,\partial E} - \frac{\partial\psi}{\partial E}\frac{\partial\psi}{\partial x}\right]_{-x}^{x}. \tag{23}$$

Assuming now that the velocity at infinity is equal to $\hbar k/M_0$, we can write down the asymptotic behavior of the wave function $\psi(x)$ ($x \to \pm\infty$):

$$\psi(x) = (\hbar k/M_0)^{-1/2}\,[\exp(ikx) - R(k)\exp(-ikx)].$$

$$x \to -\infty; \tag{24}$$

$$\psi(x) = (\hbar k/M_0)^{-1/2}\,T(k)\exp(ikx),\quad x \to +\infty. \tag{25}$$

The function $\psi_0(x)$ is normalized by the condition

$$\int |\psi_0|^2\, dx = |R(k)|^2/(\hbar k/M_0). \tag{26}$$

Substituting (22) and (26) in (20), we obtain

$$\Delta t(x) = -\hbar\frac{\partial\delta}{\partial E}|R(k)|^2 - \frac{\hbar|R(k)|}{2E}\sin(2kx-\delta), \tag{27}$$

where $|R(x)|$ and $\delta(x)$ are the modulus and phase of the reflection coefficient, respectively:

$$R(k) = |R(k)|\exp[i\delta(k)]; \tag{28}$$

$$|R(k)|^2 + |T(k)|^2 = 1. \tag{29}$$

Averaging (27) over a sufficiently large interval, we have

$$\langle\Delta t\rangle = -\hbar\left[\frac{d\delta}{dE}\right]|R(k)|^2. \tag{30}$$

3. PHENOMENOLOGICAL MODELS

The short de Broglie wavelength in spontaneous decays makes it possible to treat the relative motion of the two fragments, even under conditions when their surfaces overlap, as the motion of two classical particles along trajectories. These trajectories can be determined, for example, on the basis of a phenomenological Schrödinger equation with approximate boundary conditions.

A semiempirical theory of cluster decay was developed soon after the discovery of ^{14}C decay from ^{223}Ra and contains elements of the theory of α decay[26] and spontaneous fission.[27] In its framework, the original estimates (14) and (16) of the penetrability P could be related to the experimental half-lives and used to calculate the absolute lifetimes. In all the phenomenological models, a certain model is used to describe the interaction of the fragments, i.e., for the potential energy. This model contains a minimal number of parameters (which describe, for example, the elongation and formation of a neck). In addition, the mass parameters are assumed to be constant or to have a known functional form. The half-life T_c is calculated for different values of these parameters until satisfactory agreement with the experimental data is achieved. In such an approach, the question of the uniqueness of the solution of the Schrödinger equation is simply not considered, and the same is true for the condition of applicability of the WKB approximation for the entire class of employed potentials.

In these models, no study is made of the microscopic structure of the unstable system during its evolution, and the structure effects are described phenomenologically.

Poenaru–Ivascu–Săndulescu–Greiner model

After the discovery[2] of spontaneous decay with emission of a ^{14}C cluster from ^{223}Ra, attempts were immediately made to calculate the half-life for this decay and for other possible decays.[21–25] The authors of these studies showed that the analysis of the experimental lifetimes can be approached purely phenomenologically by assuming that the α-particle approach is manifested in the Geiger–Nuttall law and that this law can be directly generalized to cluster decay.

For cluster decay, as for α decay and fission,[35,36] the

lifetimes were calculated by means of the relation (19), in which $F = 1$:

$$T = \frac{\ln 2}{nP}, \tag{31}$$

where $n = \omega/2\pi$ is the number of collisions with the barrier in 1 sec (the characteristic frequency of the collective mode that leads to the cluster decay), $\hbar\omega/2 = E_0$ is the energy of the zero-point vibrations, and P is the probability of passage through the barrier.

In accordance with the semiclassical one-dimenisonal theory,

$$P = \exp\left\{-\frac{2}{\hbar^2}\int_{r_1}^{r_2}[2M(r)(V(r)-E)]^{1/2}\,dr\right\}, \tag{32}$$

where $E = Q + E_0$, Q [see Eq. (1)] is the decay energy, $M(r)$ is a mass parameter, taken to be $M = A_1A_2/(A_1 + A_2)$, $V(r)$ contains Coulomb, nuclear, and centrifugal terms [like (9)] and a term that describes the phenomenological shell correction δV_{sh},

$$V(r) = V_{\text{Coul}}(r) + V_{\text{nuc}}(r) + V_{\text{cent}}(r) + \delta V_{\text{sh}}, \tag{33}$$

and r_1 and r_2 are the turning points: $V(r_1) = V(r_2) = E$. For the description of V_{Coul}, the following approximate formula was used:

$$V_{\text{Coul}}(r) = \begin{cases} \alpha(3/2 - r^2/R_T^2)/R_T & \text{for } r < R_T; \\ \alpha/r & \text{for } r > R_T, \end{cases} \tag{34}$$

where $R_T = R_1 + R_2$, R_1 and R_2 are the radii of the spherical fragments, and $\alpha = Z_1Z_2e^2$.

The nuclear term V_{nuc} was described by various means: a Woods–Saxon potential with parameters determined from the elastic scattering of the heavy ions;[1,38] a potential of finite-range nuclear forces;[22,39] a Yukawa potential and an exponential interaction[20-40] ($r > R_T$), and an analytic potential calculated by means of a polynomial of second degree in r:[23-25]

$$V_{\text{nuc}}(r) = Q + (E - Q)[(r - R_i)/(R_T - R_i)]^2; \quad r \leqslant R_T, \tag{35}$$

where $R_i = r_0A^{1/3}$, $R_1 = r_0A_1^{1/3}$, $R_2 = r_0A_2^{1/3}$.

This last potential was used in practice in most calculations. It should be noted that in this model the barrier for decay and the limits of integration are determined approximately on the basis of physical or intuitive assumptions. Usually, the action integral (32) is divided into two terms, and for $\log T$ we obtain in the potential (35)

$$\log T = 0{,}43429\,(K_{0v} + K_s) - \log E_0 - 20{,}8436, \tag{36}$$

where K_{0v} and K_s depend in a complicated manner on the charge, mass, and radius of the fragments, the barrier height, and the decay energy:

$$a = b\,(E_0/E_b)^{1/2}; \quad b = R_T - R_i; \tag{37}$$

$$K_{0v} = 0{,}2196\,(E_bA_1A_2/A)^{1/2} \times\left\{(b_2 - a^2)^{1/2} - \frac{a^2}{b}\ln\left[\frac{b + (b^2 - a^2)^{1/2}}{a}\right]\right\}; \tag{38}$$

$$K_s = 0{,}4392\,(EA_1A_2/A)^{1/2}\,r^2\varphi_{mc}, \tag{39}$$

$$\varphi_{mc} = (c + m - 1)^{1/2} - [r(c - r) + m]^{1/2} + \frac{c}{2}\left[\arcsin\frac{c - 2r}{(c^2 + 4m)^{1/2}} - \arcsin\frac{c - 2}{(c^2 + 4m)^{1/2}}\right] + \sqrt{m}\ln\left\{\frac{2\sqrt{m}\,[r(c - r) + m]^{1/2} + cr + 2m}{r\,[2\sqrt{m}(c^2 + m - 1)^{1/2} + c^2 + 2m]}\right\}; \tag{40}$$

where $m = r^2E_0/E$, $c = rE_c/E$, $r_0 = 1.2249$ fm.

Parameters of this model are the radii of the final fragments, R_1 and R_2, and the energy E_0 of the zero-point vibrations. Choosing[22-25]

$$E_0 = Q\left[0{,}056 + 0{,}039\exp\left(\frac{4 - A_2}{2{,}5}\right)\right], \tag{41}$$

we obtain a significant increase of the energy E and a significant increase of the penetrability (32). For this reason, E_0 can be regarded as the main parameter of this model.

Important results, obtained in several studies (Refs. 21–25, 41, and 42), are given in Figs. 7–10. We note here that the lifetime with respect to cluster decay depends strongly on the details of the barrier and on the shell effects. Systematic study of the cluster decay in this model showed that the discrepancy with the experimental data increases with increasing mass of the emitted cluster.

In Ref. 41, this approach was generalized for deformed fragments. In this case, it was shown that the barrier is decreased for prolate deformations and increased for oblate deformations.

Finally, some details of this model were refined in Refs. 43–45. They include the use of a variable mass parameter

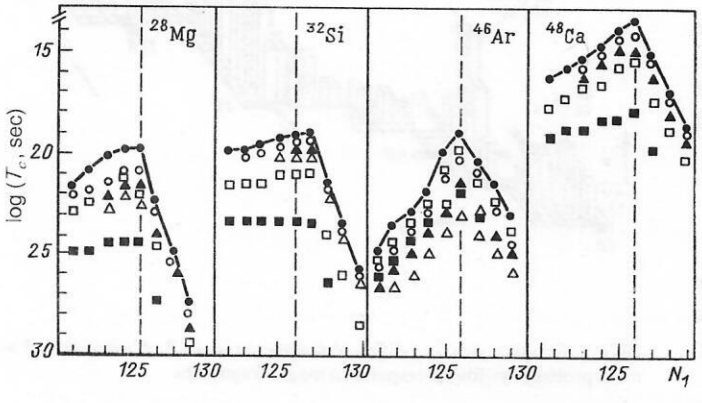

FIG. 7. Dependence of T_c on the neutron number N_1 of the heavy fragment for emission of the nuclei ^{28}Mg, ^{32}Si, ^{46}Ar, and ^{48}Ca. The proton numbers Z_1 of the daughter nucleus are as follows: 80 (black squares), 81 (open squares), 82 (black circles), 83 (open circles), 84 (black triangles), and 85 (open triangles). Even–odd effects are clearly manifested in T_c, and the minimal value for T_c is obtained for a magic fragment A_1 ($Z_1 = 82$, $N_1 = 126$).

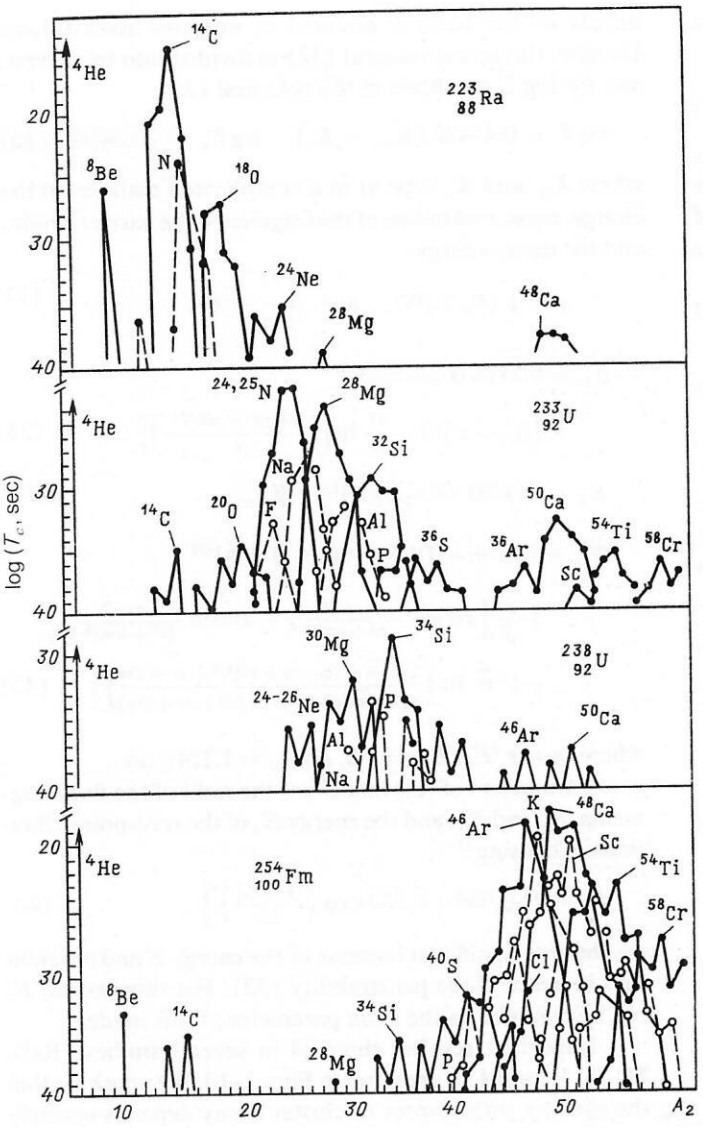

FIG. 8. Lifetimes with respect to spontaneous cluster decay, calculated on the basis of the expression (36) (Ref. 24) for the parent nuclei ^{223}Ra, ^{233}U, ^{238}U, and ^{254}Fm.

and a more detailed description of the even–odd structure and shell effects. Detailed study of the cluster decay showed that it is a general phenomenon and that the decay probabilities are high for magic numbers of the protons and neutrons ($Z = 28$, 50, 82 and $N = 28$, 50, 82, 126). The different regions of masses in which cluster decay can be expected are shown in Fig. 9.

Shi–Swiatecki model

Shi and Swiatecki[46] used the WKB method to calculate the probability of penetration P using a constant mass parameter, $M(r) = M_0$, and a contact potential $V_p(z)$ as the nuclear potential (9). As in the case of (14), they obtained

$$P = \exp\{0{,}4374\, b\, (A_1A_2/A)^{1/2} \int_{x_0}^{x} [V(x)]^{1/2}\, dx\} \quad (42)$$

where $b = 1$ fm, $r = L - C_1 - C_2$ is the distance between the centers of the fragments, C_1 C_2 are the central radii of the fragments, $L = L_c = 2(C_1 + C_2)$ corresponds to the fragments in contact, $Z = xb$, and

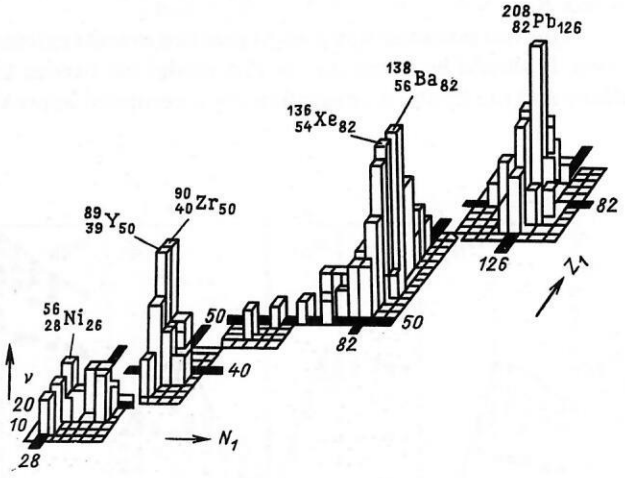

FIG. 9. Relative yields of different fragments in a (Z, N) diagram. The most probable yields correspond to magic fragments.

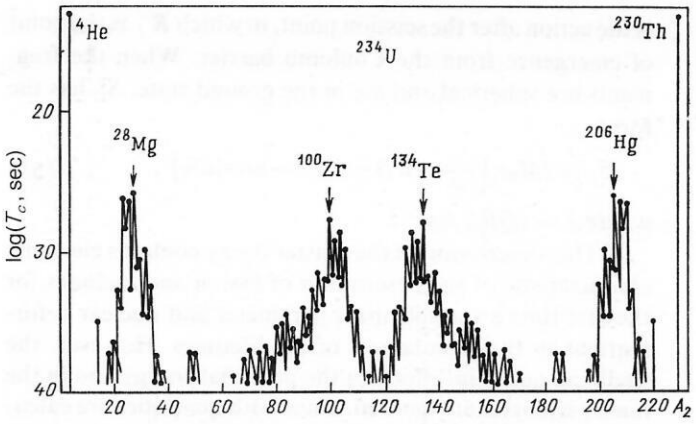

FIG. 10. Dependence of the partial lifetimes of α decay, cluster decay, and cold fission of the ^{234}U nucleus on the mass of the emitted cluster. The more probable cluster decays $^{24-26}$Ne and ^{28}Mg predicted by Poenaru and Ivascu[43] were found by the group of Price *et al.*[14]

$$V(L)=\begin{cases} Z_1Z_2e^2/r+V_p(z)-Q; & L>L_c, \\ a(L-L_0)^\nu, & L_0<L<L_c. \end{cases} \quad (43)$$

The constants a and ν in (43) are determined from the condition of continuity of $V(L)$ at $L=L_c$.

The half-lives are determined by means of the periods of the internal motions (in order of magnitude, 10^{-22}–10^{-21} sec):

$$T_\alpha = r_0^\alpha P_\alpha; \quad (44)$$

$$T_c = r_0^c P_c. \quad (45)$$

Because $r_0^\alpha \approx r_0^c$, we obtain from (44) and (45)

$$B = P_\alpha/P_c. \quad (46)$$

This method was generalized[47] to the case of deformed fragments. The results obtained with allowance for the nuclear deformations and shell corrections[47] and without them[46] are shown in Fig. 11. It is evident that inclusion of deformation and shell corrections leads to better agreement with the experimental data.

Pik-Pichak model

It was shown by Pik-Pichak[48] that by the introduction of a coordinate analogous to a fission degree of freedom one can give a good description of cluster decay even in the one-dimensional Gamow approximation. The physical coordinate in the model of Ref. 48 is the distance between the centers of mass of the fragments (Fig. 12).

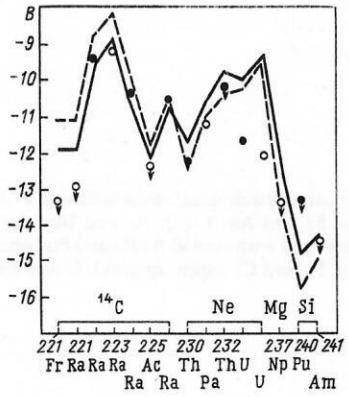

FIG. 11. Calculated values of $B=\log(T_\alpha/T_c)$.[47] The broken line represents the results of calculation for spherical fragments and without shell corrections; the continuous line represents the results of calculation for deformed fragments with allowance for shell corrections.

The below-barrier path with respect to the coordinate R_L (from the parent nucleus to the scission point), equal to

$$\Delta R_L = R_1 + R_2 - (A_1/A_2)(R - R_2),$$

is found to be much shorter than in the case of the α-decay approach.[24] For example, for the decay $^{223}\text{Ra}\rightarrow{}^{14}\text{C}+{}^{209}\text{Pb}$, $\Delta R = 4.449$ fm when the description of Ref. 24 is used and $\Delta R_L = 3.175$ fm in the case of the fission description of Ref. 48, and, therefore, the latter value is more appropriate (moreover, in this case the action up to the scission point is significantly reduced).

In Ref. 49, the mass parameters were estimated in the framework of a hydrodynamic approximation. The potential energy was determined by the interaction of a prolate (or oblate) ellipsoid and a sphere:

$$V(R_L)=\frac{3}{2}\frac{\alpha}{R_1(c_1^2-1/c_1^2)^{1/2}} \times\left\{\frac{1-\nu^2}{2}\ln\frac{\nu+1}{\nu-1}+\nu\right\}-Q;\ R_L\geqslant R_L^p, \quad (47)$$

where $\nu = R_L/[R_1(1/c_1^2 - c_1^2)]$, $\alpha = Z_1Z_2e^2$, Q is the decay energy, R_1 is the mean radius of the heavy nucleus (the major axis along the direction of separation), and R_L^p is the distance at the scission point.

For an oblate ellipsoid, for which the minor axis is directed along the axis of separation,

$$V(R_L)=\frac{3}{2}\frac{\alpha}{R_L}\{\nu(1+\nu^2)\arctan\nu^{-1}-\nu^2\}-Q;\ R_L\geqslant R_L^p, \quad (48)$$

where $\nu = R_L/[R_1(1/c_1 - c_1)]$.

Up to the scission point, the interaction potential is approximated by a sum of a cubic parabola and an ordinary parabola:

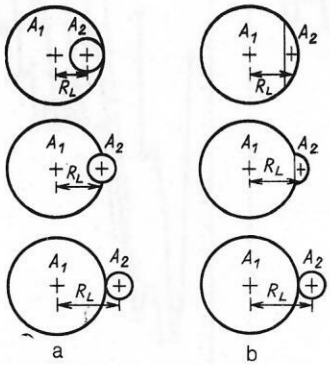

FIG. 12. Parametrization of the process of cluster decay: a) taking place as α decay (Refs. 21–24); b) taking place as a fission process.[48]

is found to be much shorter than in the case of the α-decay approach.[24] For example, for the decay $^{223}\mathrm{Ra} \rightarrow {}^{14}\mathrm{C} + {}^{209}\mathrm{Pb}$, $\Delta R = 4.449$ fm when the description of Ref. 24 is used and $\Delta R_L = 3.175$ fm in the case of the fission description of Ref. 48, and, therefore, the latter value is more appropriate (moreover, in this case the action up to the scission point is significantly reduced).

In Ref. 49, the mass parameters were estimated in the framework of a hydrodynamic approximation. The potential energy was determined by the interaction of a prolate (or oblate) ellipsoid and a sphere:

$$V(R_L) = -E_\nu + (E_{\text{Coul}} + E_\nu - Q) f(k, p), \qquad (49)$$

where $f(k, p) = (1 + k)p^2 - kp^3$, E_{Coul} is the Coulomb potential at the time of scission; $R_L = R_L^p$, $p = (R_L - R_L^{\text{in}})/(R_L^p - R_L^{\text{in}})$, R_L^{in} is the initial distance between the centers of mass of the fragments in the parent nucleus, and $E_\nu = 2$ MeV is the energy of the zero-point vibrations of the fission degree of freedom. The main calculations of the lifetimes for cluster decay were made with $k = 1$ and $p = 1$ [$f(k, p)$ is identical for a sphere and for a deformed nucleus].

In the semiclassical approximation, one can solve Eq. (10) with a potential energy (47) [or (48)] and (49), and determine the barrier penetrability $P = [\varphi(R_L^p)/\varphi(R_L^{\text{in}})]^2$, from which it follows that[48]

$$\ln T = \ln\left[2\pi (M_0/c)^{1/2} \left(\frac{2}{\hbar} S_N + \frac{2}{\hbar} S_C\right)\right], \qquad (50)$$

where

$$S_N = \int_{R_L^{\max}}^{R_L^p} [2M(R_L)V(R_L)]^{1/2}\, dR_L \qquad (51)$$

is the semiclassical action below the barrier in the region in which the nuclear forces act, and

$$S_C = \int_{R_L^p}^{R_L^c} [2M_0 V(R_L)]^{1/2}\, dR_L \qquad (52)$$

is the action after the scission point, in which R_L^c is the point of emergence from the Coulomb barrier. When the fragments are spherical and are in the ground state, S_C has the form

$$S_C = 2M_0\alpha\left\{\frac{\pi}{2\lambda} - \lambda(1-\lambda)^{1/2} - \arcsin\lambda\right\}, \qquad (53)$$

where $\lambda = (QR_L^p/\alpha)^{1/2}$.

This description of the cluster decay contains elements characteristic of the description of fission and includes for the first time a variable mass parameter and nuclear deformations in the calculations of the lifetimes. However, the shell and quantum effects in the potential energy and in the mass parameter are ignored. Since both quantities are calculated approximately, it is entirely possible that the errors compensate each other. The calculated results agree well with the experimental data (Fig. 13) despite a number of schematic approximations for the mass parameter and the potential energy. We note here that the potential energy is not calculated in the center-of-mass system, and the mass parameter is too small, as in the case of spontaneous fission.[55,56]

Simplified models[49–52]

In all these simplified models, the mass parameter is assumed to be constant, $M(r) = M_0$, and the potential energy $V(r)$ (9) is determined approximately as a potential well plus the Coulomb potential,[49] the Coulomb potential plus the centrifugal potential,[50] and the nuclear potential plus the Coulomb potential.[51,52] In all these models, analytic expressions are obtained for the lifetimes, and these are helpful for studying various aspects of cluster decay.

Shanmugan–Kamalaharam model

In Ref. 53, a one-dimensional model of cluster decay is developed in complete analogy with elementary fission theory. The functional dependence of the mass parameter on the distance is chosen as in spontaneous fission:[55]

$$M(r) = M_0 + Kf(r)(M_r^i - M_0), \qquad (54)$$

where $K = 16$ (for cluster decay, in contrast to fission, for which $K = 11$),

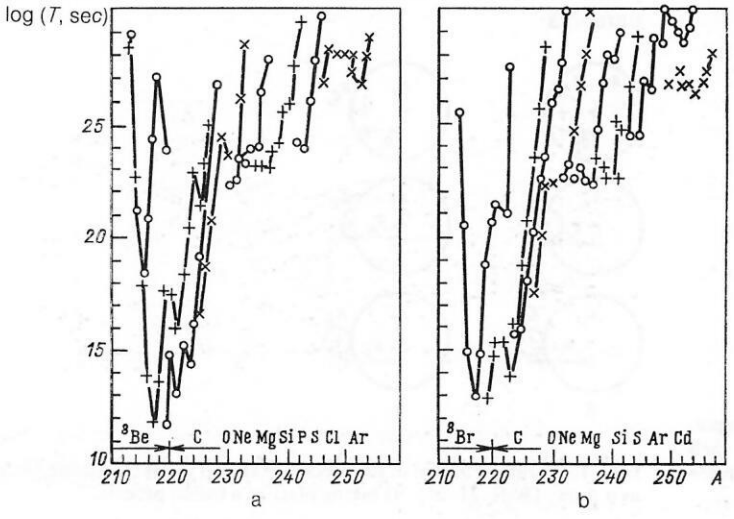

FIG. 13. Lifetimes for the most probable decay mode with odd Z: a) At and Np (open circles); Fr and Am (+); Ac and Bk (open squares); Pa and Es (crosses) and with even Z: b) Ra and Pu (open circles); Rn and Cm (+); Th and Cf (open squares); U and Fm (crosses).

TABLE II. Experimental and calculated lifetimes. The calculated values were obtained in the framework of phenomenological models.

Decay	E, MeV	log (T_c, sec)					
		Experiment	Calculation				
			Ref. 24	Ref. 47	Ref. 48	Ref. 53	Ref. 49
^{221}Fr (^{14}C)	29,28	15,77 [6]	14,4	16,0	16,5	14,5	15,2
^{221}Ra	30,34	14,35 [7]	14,3	14,8	14,7	13,3	14,1
^{222}Ra	30,97	11,02±0,06 [6, 8]	11,2	11,6	13,3	11,8	11,2
^{223}Ra	29,85	15,2±0,05 [2, 6]	15,2	15,7	15,6	14,2	15,0
^{224}Ra	28,63	15,9±0,12 [6]	15,9	16,8	18,0	17,0	16,0
^{225}Ac	28,57	18,34 [7]	17,8	19,7	19,0	18,3	18,7
^{226}Ra	26,46	21,33±0,2 [7, 8]	21,0	22,2	22,9	25,5	21,0
^{231}Pa (^{23}F)	46,68	24,61 [10]	25,9	25,5	23,4	—	26,0
^{230}Th (^{24}Ne)	51,75	24,64±0,07 [9]	25,3	24,9	26,1	25,2	24,8
^{232}Th (^{26}Mg)	49,70	27,94 [43]	28,8	28,4	29,6	29,4	29,1
^{231}Pa	54,14	23,38±0,08 [10]	23,4	23,5	23,4	22,3	23,7
^{232}U	55,86	21,06±0,1 [11]	20,8	20,0	21,8	20,6	20,7
^{233}U	54,27	24,82±0,16 [12, 13]	24,8	24,8	24,4	23,6	24,9
^{233}U (^{25}Ne)	54,32	[15]	25,0	24,4	24,4	23,6	25,1
^{234}U (^{24}Ne)	52,81	25,25±0,05 [14—16]	26,3	25,7	26,4	26,4	25,8
^{234}U (^{26}Ne)	52,87	[15]	26,5	25,0	26,4	76,5	26,2
^{234}U (^{28}Mg)	65,26	25,75±0,06 [14—18]	25,8	25,7	26,4	28,8	25,4
^{237}Np (^{30}Mg)	65,52	27,27 [9]	27,5	27,7	27,7	26,8	28,3
^{238}Pu (^{28}Mg)	67,00	25,70±0,25 [17]	25,7	24,6	26,4	25,7	25,9
^{238}Pu (^{30}Mg)	67,32	25,90±0,75 [17]	26,0	—	26,4	25,4	25,5
^{238}Pu (^{32}Si)	78,95	25,3±0,16 [17]	25,1	—	26,4	25,5	25,7
^{241}Am (^{34}Si)	80,60	25,3 [9, 18, 19]	24,5	26,2	25,5	23,8	26,5

$$f(r)=\begin{cases}[(r_t-r)/(r_t-r_i)]^4, & r<r_t=R_1+R_2;\\ 0, & r\geqslant R_T;\end{cases}$$

$$M_r^i=M_0+\frac{17}{13}M_0\exp\left[-\frac{128}{51}\left(\frac{r-r_i}{R_0}\right)\right] \qquad (55)$$

is a hydrodynamic mass parameter, and r_i is the distance between the centers of mass, which is determined by means of the heights h_i of the spherical fragments:

$$r_i=\frac{3}{4}\left(\frac{h_i^2}{R_0+h_1}+\frac{h_i^2}{R_0+h_2}\right);\ R_0=r_0A^{1/3}.$$

The potential $V(r)$ is chosen in the form

$$V(r)=\begin{cases}\alpha/r-D\left[F+\frac{r-r_t}{a}\right]\frac{r_t}{r}\exp\left[(r_t-r)/a\right]\\ \qquad\qquad\qquad\qquad\text{for}\quad r>r_t;\\ -E_v+(V(r_t)+E_v)\left[S_1\left(\frac{r-r_i}{r_t-r_i}\right)^2\right.\\ \qquad\left.-S_2\left(\frac{r-r_i}{r_t-r_i}\right)^3\right],\quad r\leqslant r_t,\end{cases} \qquad (56)$$

where D and F are two constants that depend on Z, A, R_1, and R_2, while the constants S_1 and S_2 are determined from the conditions of continuity of $V(r)$ and $V'(r)$ at $r=r_t$.

Note that (56) does not contain a centrifugal term.

Substituting (54) and (56) in (14), we obtain

$$T=\frac{1{,}433\cdot10^{21}}{E_v}[1+\exp K],$$

$$K=\frac{2}{\hbar}\int_{r_1}^{r_2}[2M(r)V(r)]^{1/2}dr; \qquad (57)$$

where

$$V(r_1)=V(r_2)=0.$$

In a certain sense, the approximation (57) makes it possible to refine the one-dimensional model of Ref. 48. The results obtained for T agree with the experimental data (Table II) to within an order of magnitude.

If we compare the values of T obtained in Refs. 53 and 48, we can note that the latter are always 1–2 orders of magnitude greater than the former. Basically, this reflects the difference between the effective mass parameters (54) and the hydrodynamic mass parameters[55,56] in the decay process. It is evident that the largest values for $M(r)$ (Ref. 53) in the initial stage of decay lead to a decrease of the barrier and of the half-life.

Potential energy and decay dynamics

A general description of the phenomenon of cluster decay in the framework of fragmentation theory was first presented in final form in Ref. 54. The potential energy is described by means of a two-center model, and the cranking model is used to calculate the mass parameters. In a two-dimensional representation [R, η, where R is the distance between the centers of mass and $\eta=(A_1-A_2)/A$ is the mass-asymmetry coordinate], the potential energy contains

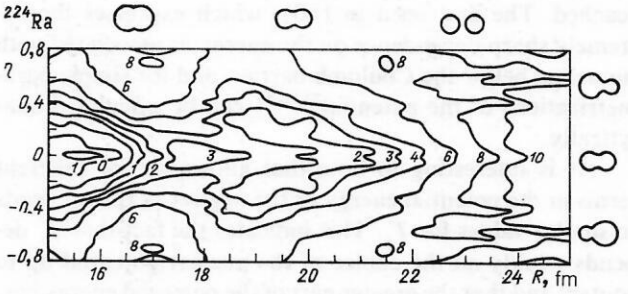

FIG. 14. Two-dimensional contours of the potential energy of the ^{224}Ra nucleus. The ground states correspond to $\eta=0$ and elongated deformations with respect to R. For large values of R cluster valleys close to the fission valleys appear.

a macroscopic term V_{ldm}, shell corrections δU, and corrections δP due to pairing effects:

$$V(R, \eta) = V_{\text{ldm}}(P, \eta) + \delta U(R, \eta) + \delta P(R, \eta). \quad (58)$$

In practical calculations, statistical quadrupole and octupole deformations are taken into account in the first term of (58).

Figure 14 shows $V(R, \eta)$ for ^{224}Ra with the V_{ldm} parameters of Ref. 38. The shell and pairing corrections were calculated approximately in the two-center model.[57] It can be seen from Fig. 14 that the ground-state barrier goes over continuously into valleys that correspond to definite shell corrections and mass asymmetries.[54,93] Such structures must be manifested in the experimental data.

Solving Eq. (10) for the ground state $\psi_0(R,\eta)$, we can determine the probability for formation of a cluster configuration characterized by the parameter η:

$$F(\eta) = \int dR \, |\psi_0(R, \eta)|^2. \quad (59)$$

It was shown that the decay dynamics is completely determined by the valley structure of the barrier (58). Unfortunately, the potential energy for extreme asymmetric fission, including cluster decay, is determined only approximately. Complete calculations of the lifetimes for cluster decay have not yet been made.

Brief review of the results of phenomenological studies. Comparison with experiment

At the present time, it is not easy to get an overall picture of the numerous phenomenological studies devoted to cluster decay. The difficulty is due not only to the large number of studies in this field, the number of which has increased strongly since 1984, but also to the different approaches to the problem. In practically all studies, the penetrabilities have been calculated in the WKB approximation and its simplified versions. The inadequacy of the WKB penetrability for the description of cluster decay when excitation of collective levels of the fragments is taken into account has now been demonstrated in several theoretical studies.

Despite the different approaches, each model[24,46-53] is a generalization of the Geiger–Nuttall law to cluster decay:

$$\log T = AQ^{-1/2} + B, \quad (60)$$

where the constant A is related to the semiclassical action, and the constant B (the pre-exponential factor) is related to internal processes that take place before the scission point is reached. The first term in (60), which expresses the extremely sharp dependence on the energy, is associated with tunneling below the Coulomb barrier, and for simple parametrizations of the potential[24,46,48] can be calculated analytically.

It is interesting to note that allowance for different terms in the potential energy or the neglect of them[50] leads to similar values for T_c. This indicates the fact that T_c depends weakly on the choice of the nuclear potential up to contact and that the greater part of the potential energy corresponds to the configurations of the already separated fragments.[25,46] The possibility of obtaining qualitatively the same agreement with experiment (see Table V) for different parameters of the nuclear potentials does not mean that the

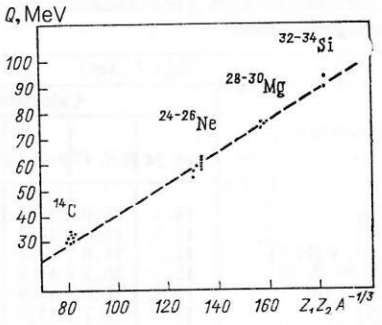

FIG. 15. Dependence of the decay energy Q on the parameter $Z_1 Z_2 A^{-1/3}$. The different cluster decays correspond to the following neutron numbers of the light nucleus: $N_2 = 8$ (^{14}C), 14 (^{24}Ne), 16 (^{28}Mg), and 20 (^{34}Si).

employed parameters correspond to reality. In other words, there is a certain arbitrariness in the determination of the geometry of this potential. It should be said that experimental scattering data do not uniquely determine the parameters of this potential.

However, the study of cluster decay in the various models did make it possible to clarify some characteristic properties of cluster decay and initiated the development of general schemes for investigating the dynamics of the process on the basis of a collective surface potential.

As a result of phenomenological analysis of cluster decay, extensive spectroscopic information has been obtained. It has been shown that large shell effects are manifested in the decay energy (see Fig. 1), in the potential energy[52] (see Fig. 14), and in the mass parameters,[52,53] and, therefore, in the lifetimes (see Figs. 7–10), especially when the fragments are magic nuclei.

As we see in Fig. 8, T_c is not a smooth function of the mass number N_1 and at certain values exhibits a "fine structure." This fine structure is due to shell effects in the products of the cluster decay (as in the case of spontaneous fission). We note that T_c is anomalously small for $A_2 = A_1$ and anomalously large for $A_2 = A_1 + 1$, $A_2 = A_1 + 2$, etc., where A_1 are magic fragments.

The most strongly expressed fine-structure peak is situated at $A_1 = 208$ ($Z_1 = 82$ and $N_1 = 126$) and $A_2 = 14$, 24, 28, 34 ($N_2 = 8$, 14, 20).

It can be seen in Fig. 15 that for $N_2 = 8$, 14, 20 the experimental decay energy Q has clear peaks, which are related to the filling of neutron shells. At such values of N_2 minima must also appear in the potential energy (see Fig. 14).

Even–odd effects in cluster decay was studied in detail in Refs. 25 and 47. The phenomenological approach [based on the expression (60)] proved to be successful.

As can be seen from Fig. 16 and Table II, the α-particle approach (and the Geiger–Nuttall law) is strongly manifested in the experimental data on T_c, particularly for light clusters (see Fig. 18).

The experimental data on cluster decay do not exhibit a "fission dependence" on the fissility parameter (Fig. 17), and the decay rate decreases with increasing fragment mass. However, the experimental values of T_c are close to the fission lines (Fig. 18).

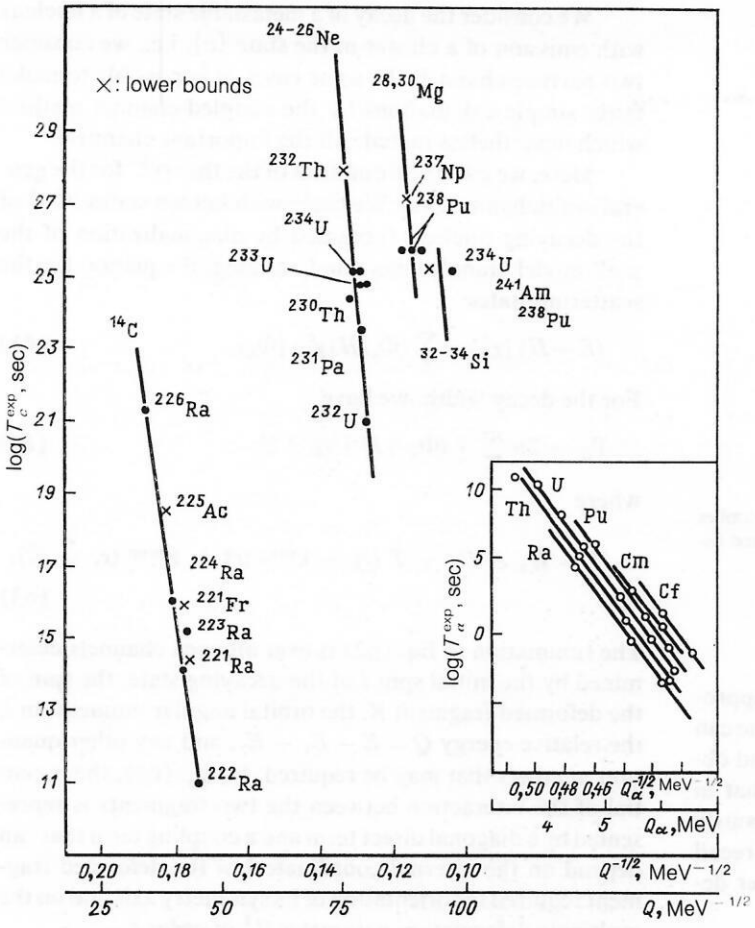

FIG. 16. Dependence of the lifetime on the decay energy. The Geiger–Nuttall law for α decay is shown on the right. The experimental data are taken from the table and Ref. 96.

4. MICROSCOPIC MODELS

The microscopic methods presented recently for analysis of cluster decay are intimately related to the well-known methods of the resonance theory of nuclear reactions. These methods provide the most general and fully developed approach for study and understanding of decay processes. In this section, we shall briefly recall the methods that make it possible to describe cluster states as sharp resonances by means of certain assumptions about the (resonance) nature of the nuclear potential. We shall obtain a general expression for the width of one resonance level (or formula for a virtual level). This formula was applied to α decay and cluster decay in a number of studies (Refs. 58–60 and 61–64).

In the microscopic approaches, the decay can be regarded as due to two main (dependent) processes: the formation of a cluster of nucleons and penetration through the barrier. The results of the Gamow models can be obtained

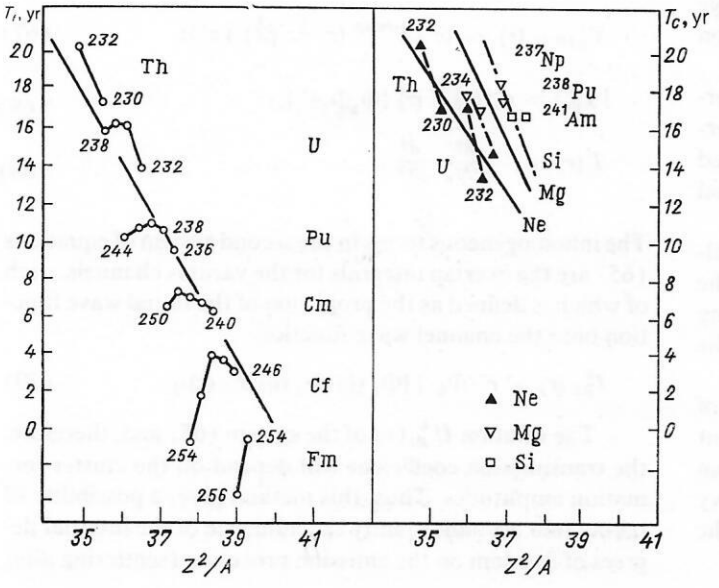

FIG. 17. Dependence of the experimental lifetimes on the fissility parameter in the case of spontaneous decays: on the left, fission; on the right, cluster decay.

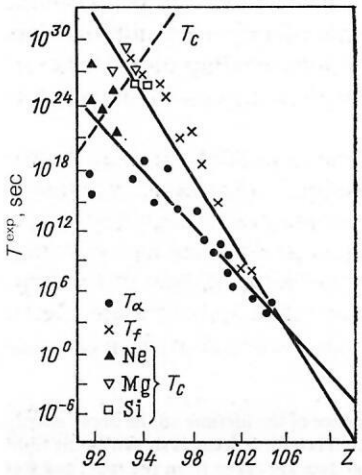

FIG. 18. Dependence of the experimental lifetimes on the proton number of the parent nucleus for cluster decay (see Table II), α decay, and fission.[96]

fairly easily from the microscopic schemes by using appropriate simplifications for the formation factor. Thus, one can make a microscopic–macroscopic analysis of decay and obtain valuable spectroscopic information. It is clear that in such an analysis it is necessary to construct simultaneously many-particle and single-particle decay models. We recall briefly the many-particle versions proposed for cluster decay.

The fact that cluster decay must be treated from the point of view of the many-particle aspect of the internal motion of the nucleus was first pointed out in Refs. 61–64. These studies advanced ideas about the fundamental mechanism of the formation of a cluster from nucleons. The treatment that we proposed in Ref. 62 is the most general and depends less on arbitrary assumptions, which are made, for example, in other studies. Above all, it does not use the relations (14) and (19) and arbitrary channel radii (in contrast, for example, to Ref. 61).

Integral approach

The solution of the complicated problem of time evolution associated with cluster decay requires a good knowledge of the important degrees of freedom and of the distribution of the energy and angular momentum between them.

On the basis of modern data, including nuclear deformations, realistic nuclear radii, and the corresponding interaction between the decay products, we constructed detailed decay schemes that take into account excitation of rotational degrees of freedom in cluster decay.

In this section, we use the method known as the generalized optical model to derive basic equations describing the absolute rates of emission of clusters in the case of strong coupling between the rotational degrees of freedom and the orbital motion of the fragments.

In what follows, we shall restrict ourselves to the case of greatest practical importance, when the emitted fragment has axisymmetric deformation and the daughter nucleus can still be regarded as spherical. This can occur when the heavy fragment is a doubly magic nucleus (usually, $^{208}_{82}$Pb), and the light cluster can have appreciable deformation.

We consider the decay of a metastable state of a nucleus with emission of a cluster in the state $\{c\}$, i.e., we consider two-particle channels. In some cases, it is possible to make fairly simple calculations by the coupled-channel method which nevertheless include all the important channels.

Here, we give the formalism of the theory[62] for the general multichannel case. We begin with known states $|\Phi_k\rangle$ of the decaying nucleus (obtained by diagonalization of the shell-model Hamiltonian) and an integral equation for the scattering states:

$$(E-H)\,|\chi_E^c\rangle = \sum_k \langle\Phi_k|H|\chi_E^c\rangle\,|\Phi_k\rangle. \tag{61}$$

For the decay width, we have

$$\Gamma_k = 2\pi \sum_c |\langle\Phi_k | H | \chi_E^c\rangle|^2, \tag{62}$$

where

$$H = H_1 + H_2 + T(r) + V^{\text{diag}}(r) + V^{\text{coup}}(\mathbf{r}, \hat{s}, \beta_i^L). \tag{63}$$

The summation in Eq. (62) is over all open channels determined by the initial spin I of the decaying state, the spin of the deformed fragment R, the orbital angular momentum l, the relative energy $Q = E - E_1 - E_2$, and any other quantum numbers that may be required. In Eq. (63), the potential of the interaction between the two fragments is represented by a diagonal direct term and a coupling term that can depend on the internal coordinate $\hat{s}$ of the deformed fragment required for orientation of its symmetry axis and on the multipole deformation parameter β_i^L of order L.

Substitution of (63) in Eq. (1) and projection onto the channel state $|c\rangle \equiv [\Phi_1\Phi_2 Y_l]_I$ give the usual equations of the coupled-channel method:

$$[T(r) + V_{Rl}(r) - Q_{Rl}]\,U_{Rl}^{0(k)}(r) - \sum V_{Rl\,R'l'}(r)\,U_{R'l'}^{0(k)}(r) \tag{64}$$

$$= \begin{Bmatrix} 0 \\ I_{Rl}^k(r) \end{Bmatrix}, \tag{65}$$

where we have used the notation

$$V_{Rl}(r) = \langle c \mid V^{\text{diag}}(r) \mid c\rangle; \tag{66}$$

$$V_{RlR'l'}(r) = \langle c \mid V^{\text{coup}}(r, \hat{s}, \beta_i^L) \mid c'\rangle; \tag{67}$$

$$|\chi_E^{Rl}\rangle = r^{-1}U_{Rl}^{0(k)}(r)\,[\Phi_1\Phi_2 Y_l]_I; \tag{68}$$

$$T(r) = -\frac{\hbar^2}{2M_0}\frac{d^2}{dr^2}. \tag{69}$$

The inhomogeneous terms in the second system of equations (65) are the overlap integrals for the various channels, each of which is defined as the projection of the initial wave function onto the channel wave function:

$$I_{Rl}^k(r) = r\,\langle\Phi_k \mid [\Phi_1(\xi)\,\Phi_2(\eta)\,Y_l(\hat{r})]_I\rangle. \tag{70}$$

The solution $U_{Rl}^k(r)$ of the system (65) and, therefore, the transmission coefficient will depend on the cluster-formation amplitudes. Thus, this method gives a possibility of taking into account exactly the influence of the internal degrees of freedom on the emission processes (scattering after

passage through the point of separation of the two fragments). Moreover, the equations of motion (64) and (65) make it possible to understand the formation stage as part of the phenomenon of penetration through the barrier.

We can solve numerically Eqs. (64) and (65) in the adiabatic approximation. In complete analogy with Ref. 62, we obtain the partial (or total) width of level k [see (70)]:

$$\Gamma_{Rl}^{k}=2\pi\left|\frac{\langle U_{Rl}^{0}(r)\,|\,I_{R}^{k}(r)\rangle}{\langle U_{Rl}^{k}(r)\,I_{R}^{k}(r)\rangle}\right|^{2}; \tag{71}$$

$$\Gamma_{k}=\sum_{Rl}\Gamma_{Rl}^{k}. \tag{72}$$

It is readily seen that the method includes averaging effects: first, over the internal (single-particle) degrees of freedom to obtain the interaction potentials (66) and (67) and the cluster-formation amplitudes [Eq. (70)] as functions of the relative distance and, second, over the relative distance in order to obtain the width from the cluster-formation amplitudes and the solution for the relative motion. Note that an arbitrarily defined radius of the nucleus is not introduced in the calculation of (62) and (72).

We emphasize that the most difficult part of the macroscopic and microscopic approximations is associated with the region that corresponds to the transition from the parent nucleus to the last contact configuration.[46,47]

In the macroscopic approach, this regime is estimated by simple tunneling through the Coulomb barrier based on empirical information on the barrier boundaries. Such information includes the frequency of collisions with the barrier, which is taken equal to the frequency of the nuclear collective oscillations, the constant reduced mass, and the model for the interaction potential.

In the microscopic approach, this corresponds to integration of the system of equations (64)–(65), the inhomogeneities of which satisfy the usual boundary conditions for bound states. Naturally, the solutions in this region form a smooth interpolation between the cluster-formation amplitudes in the ground state of the parent nucleus and the last contact configuration, when the relative wave function is equal to the asymptotic Coulomb wave function, which has the correct behavior and can be calculated exactly. The characteristic behavior of the system in this region is determined from the factorized product of the two- and four-particle microscopic amplitudes and the penetrabilities, which depend on them. For such an estimate, a hypothesis about the collision frequency is not needed, since the initial boundary conditions contain information about the period of the motion before the scission point. A problem that remains is to describe the perturbed motion when the two nuclei overlap appreciably and interact strongly with one another. By means of modern procedures, the effective mass and the nucleus–nucleus interaction can be accurately estimated, and the calculation of the contribution from the prescission configuration on the lifetime is fairly reliable.

We summarize the most important aspects of the formalism:

1. The quantum-mechanical theory of tunneling is described in the two-dimensional case (in the variables r and θ). The problem of the emission rate in the multichannel case is reduced to solution of a homogeneous and an inhomogeneous system of coupled equations, which contain microscopic formation factors.

2. By means of the adiabatic approximation, the effect of the coupling is represented as a family of potential barriers associated with the excitation modes in the process of cluster decay, some of which give rise to an increase in the penetrability.

3. In practical calculations of the lifetimes, it is possible to take into account the following factors: the deformation of the ground state in the parent nucleus through the Nilsson orbitals used to construct the cluster-formation amplitudes; the static deformation due to the interaction of the fragments near the scission point; shell and structure effects, which are contained directly in the masses of the nuclei and in the nuclear structure models.

For numerical solution of the system (64)–(65), we use the method of Numerov.[62] The advantage of this method is that the multichannel problem is reduced to a single-channel problem in which the coupling of the channels is manifested as an inhomogeneity of the (single-channel) Schrödinger equation. Below, we shall consider some approximations in the framework of the integral approach.

One-dimensional resonance approximation

The case of one resonance level with one open channel was considered in the integral approach in Refs. 62 and 66. The value of the energy in the neighborhood of which there is a resonance corresponds to the expression (1), and the single-particle eigenfunctions of the Hamiltonian (2) are determined from (64) with the condition (24)–(25).

To avoid the difficulties associated with the nonunique information about the resonance scattering of the fragments, it is necessary to do the following: a) ignore the antisymmetrization of the wave functions (5); b) ignore the effects associated with the formation of the unstable system and its excitation.

The resonance parameters can be determined by using data on the scattering of clusters by heavy nuclei (especially by the Hg, Tl, Pb, and Bi isotopes). We choose the depth of the nuclear potential V_0 as a resonance parameter in order to find an asymptotic solution of (64) and an asymptotic expansion for (79). However, it is clear that if the potential barrier is made broad or high, the scattering state $\chi_{Rl}(r)$ (68) can be transformed into one of the levels of the discrete spectrum. Therefore $|\Phi_k\rangle$ can be expanded[66] with respect to the asymptotic Coulomb functions, and as a result of this we obtain from (70) and (71)

$$I_{r}(r)=G(r); \tag{73}$$

$$\Gamma_{r}=2\pi\left|\frac{\langle U^{0}(r)\,|\,G(r)}{\langle U^{k}(r)\,|\,G(r)}\right|^{2}, \tag{74}$$

where U^0 and U^k are solutions of the system

$$[T(r)+V(r)-Q]\begin{Bmatrix}U^{0}(r)\\U^{R}(r)\end{Bmatrix}=\begin{Bmatrix}0\\G(r)\end{Bmatrix} \tag{75}$$

and $G(r)$ is a normalized irregular Coulomb function.

It follows from (74) that

$$\lambda_{r}=\frac{2\pi}{\hbar}\left|\frac{\langle U^{0}(r)\,|\,G(r)\rangle}{\langle U^{k}(r)\,|\,G(r)\rangle}\right|^{2}. \tag{76}$$

Numerical comparison of (76) with the Breit formula[67]

$$\lambda_{B}=v\left[\int_{0}^{R}|G(r)|^{2}\,dr\right]_{E_r}^{-1};\quad v=[E_r/2M_0]^{1/2} \tag{77}$$

TABLE III. Experimental and single-particle resonance widths for the emission of ^{14}C from the isotopes $^{223-224}Ra$ and ^{24}Ne from ^{231}Pa and $^{232-233}U$. The resonance widths were obtained on the basis of the expression (76). The fifth column gives the single-particle widths from Ref. 64.

Nucleus	Γ^{exp}, MeV	Γ_r, MeV	$S=\Gamma^{exp}/\Gamma_r$	Γ_0, MeV
^{222}Ra	$0{,}440\cdot10^{-32}$	$0{,}202\cdot10^{-21}$	$0{,}217\cdot10^{-10}$	$0{,}790\cdot10^{-23}$
^{223}Ra	$0{,}303\cdot10^{-36}$	$0{,}228\cdot10^{-26}$	$0{,}132\cdot10^{-9}$	$0{,}490\cdot10^{-25}$
^{224}Ra	$0{,}629\cdot10^{-37}$	$0{,}858\cdot10^{-27}$	$0{,}733\cdot10^{-10}$	$0{,}130\cdot10^{-27}$
^{226}Ra	$0{,}285\cdot10^{-42}$	$0{,}105\cdot10^{-31}$	$0{,}276\cdot10^{-10}$	—
^{231}Pa	$0{,}176\cdot10^{-44}$	$0{,}781\cdot10^{-29}$	$0{,}225\cdot10^{-15}$	$0{,}750\cdot10^{-26}$
^{232}U	$0{,}460\cdot10^{-42}$	$0{,}901\cdot10^{-27}$	$0{,}510\cdot10^{-15}$	$0{,}170\cdot10^{-24}$
^{233}U	$0{,}699\cdot10^{-46}$	$0{,}649\cdot10^{-30}$	$0{,}107\cdot10^{-15}$	$0{,}480\cdot10^{-27}$

showed that to a high accuracy the values of λ_r and λ_B are equal, $\lambda_r \equiv \lambda_B$. Note that in its form the result (77) is analogous to Gamow's result $T \sim Q^{-1/2}$ and to the first term of the Geiger–Nuttall relation (60). The only difference is that (76) and (77) were obtained for a wave function and not for a solution with complex energy (which is physically unacceptable because it leads to an infinite probability for finding the particle at large distances). Moreover, we also take into account the reflection of the incoming flux from the regions of a high barrier [see (25) and (26)].

Figure 17 gives results (T_c, T_α) for four Ra isotopes with T_c calculated by means of (76), and also experimental values (T_c, T_α).[96] We note that the pure single-particle approximation on the basis of (76) leads to very small values for T_c (on the average, ten orders of magnitude smaller than the experimental values). It is evident that when the resonance condition is satisfied the penetrability reaches large values, in contrast to the semiclassical estimates.[25,46] For the discussion of this discrepancy, some numerical examples will be helpful. Table III gives the experimental and resonance widths (74) and their ratio S (the so-called spectroscopic factor). If S_α is expressed in terms of the mean spectroscopic factor of α decay (S_α),

$$S_c = [S_\alpha]^{n_\alpha + (N_2 - Z_2)/4}, \tag{78}$$

where n_α is the number of α particles of the cluster, then for ^{14}C and ^{24}Ne emissions we obtain $S_\alpha = 10^{-2.7}$–$10^{-2.8}$, in complete agreement with the estimates of Refs. 2, 61, and 64; here $S_\alpha = \int I^2(r)dr$, and for the majority of α emitters $I(r) = 10^{-1}$–10^{-2} fm$^{-1/2}$.

Even in this elementary description it can be noted (see Fig. 17) that even–even effects are manifested (only through the decay energies).

One-dimensional shell approximation

The case of cluster decay of one resonance state from one open channel was considered for the first time in the framework of this approximation in Refs. 62 and 64. In Ref. 62 the system (64)–(65) was solved with the usual conditions for the scattering functions $U^0_{Rl}(r)$; $V_{Rl}(r)$ (66) corresponds to two charged spheres, and the nondiagonal terms of (67) are ignored, i.e., $V_{RlR'l'}(r) = 0$. The geometry of the phenomenological potential[71–73] for cluster decay is fixed by means of the condition of a resonance state (see Sec. 3).

The method of calculating the amplitudes of cluster formation[62] from individual nucleons was specially developed in complete analogy with the method of calculation of α-particle formation amplitudes.[59,60,68] The cluster-formation amplitude, i.e., $I_{Rl}(r)$ (70), is proportional to the matrix element of the cluster-production operator A^+ between the initial and final states:

$$I_{Rl}(r) = r\langle\Phi_k|\mathcal{A}[\Phi_1\Phi_2 Y_{lm}(\hat{r})]\rangle \equiv r\langle\Phi_k|\mathcal{A}[A^+(r,\ l,\ m)\,\Phi_1]\rangle, \tag{79}$$

where $\mathcal{A}$ is the antisymmetrization operator.

The cluster-formation amplitude can be found by generalizing the operator of two-nucleon transfers and the operator of α-particle production to the case of cluster formation:[68]

$$A^+(r,\ l,\ m) = \frac{1}{A_2!}\sum_{\nu_i}\langle\nu_1\ \dots\ \nu_{A_2}|\xi\Delta tlm\rangle\, a^+_{A_2}\ \dots\ a^+_1,$$

where the factor $\langle\nu_1,\dots\nu_{A_2}|\xi\Delta tlm\rangle$ is the transformation coefficient that describes the overlap between the antisymmetrized products of the single-particle oscillator[68] orbits $\nu_i r_i$ [Slater determinants for protons and neutrons $\mathcal{A}\Psi(Z_2)$ and $\mathcal{A}\Psi(N_2)$] with internal cluster function $\Phi_c(\xi\Delta t)$ and relative-motion function $Y_{lm}(r)$, i.e.,

$$\langle\nu_1\ \dots\ \nu_{A_2}|\xi\Delta tlm\rangle = C^{ZN}_{Z_2N_2} \times \int d\Omega_{\hat{r}}\, d\xi\, \mathcal{A}\Psi(Z_2)\,\mathcal{A}\Psi(N_2)\,\Phi_c(\xi\Delta t)\,Y_{lm}(\hat{r}), \tag{80}$$

in which $C^{ZN}_{Z_2N_2}$ are coefficients of fractional parentage.[82]

The cluster ground-state function Φ_c is chosen in the basis of oscillator cluster wave functions (Φ_{α_i}, Ψ_k) in the ground states:

$$\Phi_c(\xi\Delta t) = \prod_{i=1}^{n_\alpha}\Phi_{\alpha_i}\prod_{k=3n_\alpha+1}^{A_2-3n_\alpha-1}\Phi_k, \tag{81}$$

where Φ_{α_i} is the internal function of cluster α_i; the function Ψ_k describes the relative motion of two clusters (of nucleons) [$k = \{(\alpha_i\alpha_j),\ (nn),\ (\alpha(nn)),\ (\alpha\alpha(\alpha nn)),\ (\alpha\alpha(\alpha\alpha)),\dots\}$]. To each cluster representation there corresponds a complete system of antisymmetrized orthonormal oscillator functions (Φ_{α_i}, Ψ_k). This system ensures a simple description of the lowest nuclear states and permits comparison of its basis functions with the functions of the shell model and calculation of the coefficients (80). In the α-cluster representation, we use the following basis oscillator functions:[62,82]

$$\Phi_{\alpha_i}=\left(\frac{\beta}{\pi}\right)^{9/4}\exp\left[-\frac{\beta}{2}(\xi_{1\alpha_i}^2+\xi_{2\alpha_i}^2+\xi_{3\alpha_i}^2\right]x_{00}(s_{1\alpha_i}\ \dots\ t_{4\alpha_i})\times Y_{00}(\hat{\xi}_{1\alpha_i})\,Y_{00}(\hat{\xi}_{2\alpha_i})\,Y_{00}(\hat{\xi}_{3\alpha_i});$$

$$\Psi_{\alpha_i\alpha_J}=\frac{4\alpha^2}{3\sqrt{105}}\left(\frac{\alpha}{\pi}\right)^{3/4}\xi_{\alpha_i\alpha_J}^4\exp\left[-\frac{\alpha}{2}\xi_{\alpha_i\alpha_J}^2\right]Y_{00}(\hat{\xi}_{\alpha_i\alpha_J});$$

$$\Psi_{n_1n_2}=\left(\frac{\alpha}{\pi}\right)^{3/4}\exp\left[-\frac{\alpha}{2}\xi_{n_1n_2}^2\right]x(s_{n_1}t_{n_2})\,Y_{00}(\hat{\xi}_{n_1n_2});$$

$$\Psi_\alpha(nn)=\frac{2\alpha}{\sqrt{15}}\left(\frac{\alpha}{\pi}\right)^{3/4}\xi_{\alpha nn}^2\exp\left[-\frac{\alpha}{2}\xi_{\alpha nn}^2\right]Y_{00}(\hat{\xi}_{\alpha nn});$$

$$\Psi_{\alpha\alpha}(\alpha nn)=\frac{4\alpha^2}{3\sqrt{105}}\left(\frac{\alpha}{\pi}\right)^{3/4}\xi_{\alpha\alpha\alpha nn}^4\times\exp\left[-\frac{\alpha}{2}\xi_{\alpha\alpha\alpha n}^2\right]Y_{00}(\hat{\xi}_{\alpha nn});$$

$$\Psi_{\alpha\alpha}(\alpha\alpha)=\frac{4\alpha^2}{3\sqrt{105}}\left(\frac{\alpha}{\pi}\right)^{3/4}\xi_{\alpha\alpha\alpha\alpha}^4\times\exp\left[-\frac{\alpha}{2}\xi_{\alpha\alpha\alpha\alpha}^2\right]Y_{00}(\hat{\xi}_{\alpha\alpha\alpha\alpha}),\qquad(82)$$

where x is the spin–isospin part of the function, $\beta=0.47\times10^{26}\,\mathrm{cm}^{-2}$ corresponds to the mean radius of an α cluster,[68] and α is the oscillator parameter. The principal quantum number N_0 for the functions (82) takes the values $N_0=0,4;\ 0,2;\ 4,4$. Note that as a result of the antisymmetrization of these functions[82] only the terms $(\alpha\xi^2)^{n/2}$ remain from the usual Laguerre polynomials $L_{n0}(\alpha\xi^2)$. The functions Φ_{α_i} correspond to the ground states of the α clusters, and the spins and isospins of the nucleons are added to total angular momentum $s_\alpha=0$ and total isospin $T_\alpha=0$, respectively.

To calculate the coefficient (80), we must do the following. In the functions $A\Psi(Z_2)A\Psi(N_2)$ we go over from the coordinates $r_1\dots r_{A_i}$ to the internal coordinates $\xi_{1\alpha_i}$, $\xi_{2\alpha_i}$, $\xi_{3\alpha_i}$, to the coordinates R_{α_i} of the centers of mass of the α clusters, and to the relative coordinates ξ_k. Integrating over $\xi_{1\alpha_i}$, $\xi_{2\alpha_i}$, $\xi_{3\alpha_i}$ in (80) by means of the procedure of Ref. 68, we obtain analytic expressions for the cluster-formation amplitudes $I_{00}^{\alpha}(R_{\alpha i})$. Finally, going over from R_{α_i} to the cen-

TABLE IV. Values of T_c obtained in the microscopic theory of Ref. 62 for the most probable cluster decays. The experimental values of T_α and T_f are taken from Refs. 20 and 96.

Nucleus	Cluster	T_c, sec	T_c/T_α	T_f/T_α
^{230}Th	^{20}O	$0{,}470\cdot10^{26}$	$0{,}182\cdot10^{14}$	$0{,}2\cdot10^{13}$
	^{22}O	$0{,}416\cdot10^{25}$	$0{,}174\cdot10^{13}$	
	^{4}He	$0{,}239\cdot10^{13}$	—	
^{232}Th	^{20}O	$0{,}724\cdot10^{31}$	$0{,}163\cdot10^{14}$	$0{,}7\cdot10^{11}$
	^{22}O	$0{,}905\cdot10^{30}$	$0{,}239\cdot10^{13}$	
	^{4}He	$0{,}444\cdot10^{18}$	—	
^{232}U	^{26}Mg	$0{,}703\cdot10^{22}$	$0{,}709\cdot10^{12}$	$0{,}110\cdot10^{13}$
	^{28}Mg	$0{,}104\cdot10^{22}$	$0{,}104\cdot10^{12}$	
	^{30}Mg	$0{,}143\cdot10^{26}$	$0{,}144\cdot10^{15}$	
	^{32}Mg	$0{,}629\cdot10^{32}$	$0{,}634\cdot10^{22}$	
	^{4}He	$0{,}991\cdot10^{9}$	—	
^{233}U	^{28}Mg	$0{,}863\cdot10^{24}$	$0{,}181\cdot10^{12}$	$0{,}750\cdot10^{12}$
	^{30}Mg	$0{,}280\cdot10^{29}$	$0{,}679\cdot10^{16}$	
	^{32}Mg	$0{,}196\cdot10^{36}$	$0{,}412\cdot10^{23}$	
	^{4}He	$0{,}489\cdot10^{13}$	—	
^{234}U	^{28}Mg	$0{,}458\cdot10^{26}$	$0{,}558\cdot10^{13}$	—
	^{30}Mg	$0{,}157\cdot10^{28}$	$0{,}201\cdot10^{15}$	
	^{32}Mg	$0{,}197\cdot10^{30}$	$0{,}253\cdot10^{17}$	
	^{4}He	$0{,}779\cdot10^{13}$	—	
^{235}U	^{30}Mg	$0{,}586\cdot10^{36}$	$0{,}261\cdot10^{10}$	$0{,}500\cdot10^{9}$
	^{32}Mg	$0{,}365\cdot10^{32}$	$0{,}163\cdot10^{16}$	
	^{4}He	$0{,}223\cdot10^{17}$	—	
^{232}Pu	^{24}Mg	$0{,}942\cdot10^{22}$	$0{,}440\cdot10^{19}$	—
	^{26}Mg	$0{,}186\cdot10^{21}$	$0{,}869\cdot10^{17}$	
	^{28}Mg	$0{,}451\cdot10^{26}$	$0{,}164\cdot10^{23}$	
	^{30}Mg	$0{,}106\cdot10^{26}$	$0{,}495\cdot10^{22}$	
	^{32}Mg	$0{,}380\cdot10^{32}$	$0{,}177\cdot10^{27}$	
	^{4}He	$0{,}114\cdot10^{4}$	—	
^{234}Pu	^{24}Mg	$0{,}299\cdot10^{25}$	$0{,}922\cdot10^{20}$	—
	^{26}Mg	$0{,}395\cdot10^{20}$	$0{,}121\cdot10^{16}$	
	^{28}Mg	$0{,}509\cdot10^{21}$	$0{,}157\cdot10^{17}$	
	^{30}Mg	$0{,}391\cdot10^{24}$	$0{,}120\cdot10^{20}$	
	^{32}Mg	$0{,}227\cdot10^{31}$	$0{,}700\cdot10^{26}$	
	^{4}He	$0{,}324\cdot10^{5}$	—	
^{241}Am	^{28}Mg	$0{,}169\cdot10^{27}$	$0{,}414\cdot10^{16}$	$0{,}250\cdot10^{12}$
	^{30}Mg	$0{,}581\cdot10^{26}$	$0{,}163\cdot10^{16}$	
	^{32}Mg	$0{,}139\cdot10^{29}$	$0{,}390\cdot10^{18}$	
	^{4}He	$0{,}356\cdot10^{11}$	—	
^{243}Am	^{28}Mg	$0{,}511\cdot10^{30}$	$0{,}220\cdot10^{20}$	$0{,}100\cdot10^{11}$
	^{30}Mg	$0{,}144\cdot10^{30}$	$0{,}612\cdot10^{19}$	
	^{32}Mg	$0{,}398\cdot10^{31}$	$0{,}171\cdot10^{21}$	
	^{4}He	$0{,}232\cdot10^{11}$	—	
^{232}U	^{32}Si	$0{,}903\cdot10^{25}$	$0{,}911\cdot10^{15}$	$0{,}110\cdot10^{13}$
	^{34}Si	$0{,}600\cdot10^{27}$	$0{,}605\cdot10^{17}$	
	^{36}Si	$0{,}337\cdot10^{31}$	$0{,}340\cdot10^{21}$	
	^{4}He	$0{,}991\cdot10^{9}$	—	
^{233}U	^{32}Si	$0{,}856\cdot10^{29}$	$0{,}175\cdot10^{17}$	$0{,}750\cdot10^{12}$
	^{34}Si	$0{,}206\cdot10^{28}$	$0{,}421\cdot10^{15}$	
	^{36}Si	$0{,}461\cdot10^{31}$	$0{,}942\cdot10^{18}$	
	^{4}He	$0{,}489\cdot10^{13}$	—	
^{234}U	^{32}Si	$0{,}882\cdot10^{26}$	$0{,}116\cdot10^{14}$	$0{,}800\cdot10^{11}$
	^{34}Si	$0{,}902\cdot10^{25}$	$0{,}119\cdot10^{13}$	

TABLE IV. (*continued.*)

Nucleus	Cluster	T_c, sec	T_c/T_α	T_f/T_α
	^{36}Si	$0{,}385\cdot10^{29}$	$0{,}509\cdot10^{16}$	
	^{4}He	$0{,}756\cdot10^{13}$	—	
^{235}U	^{34}Si	$0{,}606\cdot10^{28}$	$0{,}271\cdot10^{12}$	$0{,}500\cdot10^{9}$
	^{36}Si	$0{,}909\cdot10^{31}$	$0{,}407\cdot10^{15}$	
	^{4}He	$0{,}223\cdot10^{17}$	—	
^{241}Am	^{32}Si	$0{,}619\cdot10^{24}$	$0{,}458\cdot10^{14}$	$0{,}250\cdot10^{12}$
	^{34}Si	$0{,}191\cdot10^{25}$	$0{,}141\cdot10^{15}$	
	^{36}Si	$0{,}244\cdot10^{31}$	$0{,}180\cdot10^{21}$	
	^{4}He	$0{,}135\cdot10^{11}$	—	
^{243}Am	^{34}Si	$0{,}783\cdot10^{25}$	$0{,}337\cdot10^{13}$	$0{,}100\cdot10^{11}$
	^{36}Si	$0{,}547\cdot10^{30}$	$0{,}233\cdot10^{19}$	
	^{4}He	$0{,}232\cdot10^{12}$	—	
^{240}Cm	^{28}Si	$0{,}777\cdot10^{28}$	$0{,}339\cdot10^{22}$	$0{,}260\cdot10^{8}$
	^{30}Si	$0{,}634\cdot10^{23}$	$0{,}276\cdot10^{17}$	
	^{32}Si	$0{,}458\cdot10^{20}$	$0{,}199\cdot10^{14}$	
	^{34}Si	$0{,}209\cdot10^{23}$	$0{,}912\cdot10^{16}$	
	^{36}Si	$0{,}338\cdot10^{28}$	$0{,}147\cdot10^{22}$	
	^{4}He	$0{,}229\cdot10^{7}$	—	
^{246}Cm	^{28}Si	$0{,}427\cdot10^{28}$	$0{,}282\cdot10^{18}$	$0{,}380\cdot10^{4}$
	^{30}Si	$0{,}405\cdot10^{21}$	$0{,}268\cdot10^{11}$	
	^{32}Si	$0{,}670\cdot10^{20}$	$0{,}443\cdot10^{10}$	
	^{34}Si	$0{,}104\cdot10^{23}$	$0{,}688\cdot10^{12}$	
	^{36}Si	$0{,}309\cdot10^{28}$	$0{,}204\cdot10^{18}$	
	^{4}He	$0{,}151\cdot10^{11}$		
^{244}Cf	^{36}S	$0{,}381\cdot10^{23}$	$0{,}334\cdot10^{21}$	—
	^{38}S	$0{,}611\cdot10^{22}$	$0{,}535\cdot10^{19}$	
	^{40}S	$0{,}642\cdot10^{24}$	$0{,}563\cdot10^{21}$	
	^{4}He	$0{,}114\cdot10^{4}$		
^{248}Cf	^{36}S	$0{,}382\cdot10^{23}$	$0{,}126\cdot10^{16}$	$0{,}370\cdot10^{6}$
	^{38}S	$0{,}110\cdot10^{23}$	$0{,}364\cdot10^{15}$	
	^{40}S	$0{,}347\cdot10^{29}$	$0{,}114\cdot10^{22}$	
	^{4}He	$0{,}302\cdot10^{8}$		
^{248}Fm	^{36}Ar	$0{,}115\cdot10^{26}$	$0{,}319\cdot10^{24}$	$0{,}100\cdot10^{4}$
	^{38}Ar	$0{,}312\cdot10^{24}$	$0{,}866\cdot10^{22}$	
	^{40}Ar	$0{,}315\cdot10^{24}$	$0{,}847\cdot10^{22}$	
	^{42}Ar	$0{,}125\cdot10^{26}$	$0{,}347\cdot10^{24}$	
	^{44}Ar	$0{,}820\cdot10^{31}$	$0{,}227\cdot10^{29}$	
	^{4}He	$0{,}360\cdot10^{2}$		
^{252}Fm	^{36}Ar	$0{,}293\cdot10^{35}$	$0{,}294\cdot10^{30}$	$0{,}530\cdot10^{5}$
	^{40}Ar	$0{,}808\cdot10^{24}$	$0{,}811\cdot10^{19}$	
	^{42}Ar	$0{,}137\cdot10^{25}$	$0{,}137\cdot10^{20}$	
	^{44}Ar	$0{,}156\cdot10^{24}$	$0{,}156\cdot10^{19}$	
	^{4}He	$0{,}996\cdot10^{5}$		

ter-of-mass coordinate r (see Ref. 62), we obtain the required integral $I_{Rl}(r)$ by numerical integration with respect to ξ_k.

In these calculations, it is particularly important to include pairing effects for the α-particle formation amplitudes. The enhancement factors for α decay for a constant pairing field[69] are included explicitly in the calculations of the cluster-formation amplitudes.

Table IV gives some results that we obtained in the framework of this approximation [the mass parameter is assumed to be constant: $M(r) = M_0$]. We note that the calculated values of T_c agree with the experimental data to within 1–1.5 orders of magnitude. The discrepancy is due above all to the use of oscillator wave functions, which usually overestimate the cluster-formation amplitudes. Another factor is the neglect of the channel coupling.

In Table IV we give the most probable processes of cluster decay for isotopes of elements from ^{232}Th to ^{252}Fm. For other even–even isotopes of a given element, the values of T_c form a dependence with a maximum. Usually, this maximum corresponds to neutron numbers $N_2 = 8, 14, 20$. Such a dependence is well known for fission, for which $N_2 = 50, 82$. The commonality of the mechanisms of cluster decay and spontaneous fission must have as a consequence a similarity in the behavior of the lifetimes.

In addition, $\log(T_c/T_\alpha)$ and $\log(T_f/T_\alpha)$ for even–even nuclei decrease linearly with increasing neutron number N_2 to a fairly good approximation.

Two-dimensional approximation. Effects of fragment deformation

The main results of the phenomenological investigations of Refs. 44 and 47 lead to the conclusion that the deformation of the fragments at the time of separation depends on their shell structure. The deformation is minimal for fragments with magic numbers. The magic effect observed in the fragment deformation also leads to a magic effect in the potential energy (see Fig. 15). A direct consequence of this circumstance is the appearance of a magic effect in the decay energy Q.

In this section, we briefly present the results of earlier studies[70] in the framework of the integral approach and represent them in a systematized form. In contrast to Ref. 47, we consider the most probable case, when the light fragment is strongly deformed and the heavy, weakly excited fragment can still be regarded as spherical (this is usually a nucleus near ^{208}Pb). The deformation parameter β_L of multipolarity L determines the shape of the fragment by means of the following equation for the radius vector of the surface:

$$R_2(\theta) = R_2[1 + \sum_L \beta_L Y_{L0}(\theta)]. \qquad (83)$$

This expression is substituted in the analytic expressions for the diagonal and nondiagonal parts of the potential $V(r, \theta)$ [$V_{Rl}(r)$ and $V_{RlR'l'}(r)$] [see Eq. (67)]. To calculate the interaction, we use a potential of Woods–Saxon type and the Coulomb potential. The interaction between the axially deformed and spherical fragments takes the form

$$V(r,\ \theta)=V_0 f\{[r-R_1-R_2(1+\beta_2 Y_2(\theta))]\, a^{-1}\} + \frac{Z_1 Z_2 e^2}{r}\left[1+\frac{3}{5}\frac{R_2^2}{r^2}\beta_2 Y_2(\theta)\right]+\frac{\hbar^2 l^2}{2M_0 r^2}, \qquad (84)$$

where f is a radial form factor of Woods–Saxon type. The nondiagonal part of the potential associated with the nuclear and Coulomb excitation can be obtained from (84) in the first approximation in β_2:

$$V^{\text{coup}}(r,\ \theta)=\beta_2 R_2\left[\frac{\partial f(r)}{\partial r}+\frac{3}{5}Z_1 Z_2 e^2\frac{R_2}{r^3}\right]Y_{20}(\theta) \qquad (85)$$

and for the matrix elements (67) we obtain

$$V^{(2)}_{RlR'l'}(r)=(i)^{l+l'}(-1)^{l+l'+R+I}[(2l+1)(2l'+1)]\, C^{l'l2}_{000}C^{R'2R}_{000} \times W(l'R'lR;\ I2)\ W(lll'l';\ 02)\left[V_0\frac{\partial f(r)}{\partial r}+\frac{3}{5}Z_1Z_2e^2\frac{R_2}{r^3}\right], \qquad (86)$$

where $C^{l'l2}_{000}$ and $W(l'R'lR; I2)$ are Clebsch–Gordan coefficients and $6j$ coefficients.

Similarly, for octupole deformations (which are often also manifested in heavy fragments, for example, in ^{208}Pb for $E_3 = 3.104$ MeV), we obtain

$$V^{(3)}_{RlR'l'}(r)=(i)^{l+l'}(-1)^{l+l'+R+I}[(2l+1)(2l'+1)]\, C^{l'l3}_{000}\, C^{R'3R}_{000} \times W(l'R'lR:\ I3)\, W(lll'l';\ 03)\left[V_0\frac{\partial f}{\partial r}+\frac{2}{7}Z_1Z_2e^2\frac{R_2^2}{r^4}\right]. \qquad (87)$$

Besides nuclear potentials of Woods–Saxon type, we also use in (84) the contact potential that was first proposed for cluster-decay calculations by Shi and Swiatecki.[47] For example, for axisymmetric deformations the interaction $V(r, \theta)$ takes the form[77]

$$V(r,\ \theta)=-4\pi\gamma\frac{C_1C_2}{C_1+C_2}\left[1-2\frac{C_1}{C_1+C_2}\beta_2Y_2(\theta)\right] \times\Phi_p[r-C_1-C_2(1+\beta_2Y_2(\theta))]+ +\frac{Z_1Z_2e^2}{r}\left[1+\frac{3}{5}\frac{R_2^2}{r^2}\beta_2Y_2(\theta)\right]+\frac{\hbar^2l^2}{2M_0r^2}, \qquad (88)$$

where γ, the coefficient for the surface energy of the nucleus, and the function Φ_p are given in Ref. 47:

$$\gamma=0{,}9517\left[1-1{,}7826\left(\frac{N-Z}{A}\right)^2\right],$$

in which N, Z, and A are the numbers of neutrons, protons, and nucleons in the initial nucleus, and Φ_p is the universal function

$$\Phi_p(\xi)=\begin{cases}-0{,}5(\xi-2{,}54)^2-0{,}0852(\xi-2{,}54)^3, & \xi<1{,}2511;\\ -3{,}437\ \exp(-\xi/0{,}75), & \xi>1{,}2511,\end{cases}$$

where $\xi = r - C_1 - C_2$ is the distance between the surfaces of the nuclei, $C_i = R_i - 1/R_i$ are the half-density radii of the nuclei, and $R_i = 1.28A_i^{1/3}$ are the radii of the nuclei in the liquid-drop model.

Note that in the procedure used above for averaging the potentials over the orientations and rotations (or vibration), the fragment maintains its orientation or shape during the penetration time, i.e., the energy of rotation (or vibration) must not be large,

$$E_{\text{curl}} < \hbar/T_c.$$

In the practical calculations we include all the important channels that can be correlated with the rotational levels of the deformed fragment. In the majority of cases, we restrict ourselves to analysis of four channels (associated with the first excited levels).

For numerical solution of the system of equations (64)–(65), we use an iterative method based on an extension of Numerov's algorithm of stepwise integration of the single-channel radial Schrödinger equation.[70] A great advantage of using this method is that the coupling between the channels is manifested as an inhomogeneity of a single-channel Schrödinger equation. Our numerical tests for cluster decay showed that in the majority of cases one needs only a

TABLE V. Values of T_c obtained in Ref. 70 on the basis of the channel-coupling method with allowance for quadrupole deformations of the nuclear and Coulomb potentials.

Decay	Q, MeV	log(T_c, sec)		
		Experiment	Calculation	
			Potential (84)	Potential (85)
^{234}U → ^{24}Ne + ^{210}Pb	58,830	25,07±0,12	25,39	24,62
^{232}U → ^{24}Ne + ^{208}Pb	62,305	21,06±0,1	21,54	20,60
^{234}U → ^{28}Mg + ^{206}Hg	74,113	25,55±0,25	25,68	25,37
^{234}Pu → ^{28}Mg + ^{206}Pb	79,152	—	21,90	21,48
^{241}Am → ^{30}Mg + ^{211}Bi	74,585	—	26,36	37,55
^{237}Np → ^{30}Mg + ^{207}Tl	75,706	27,25	27,69	26,27
^{246}Cm → ^{34}Si + ^{212}Pb	90,414	—	28,74	28,68
^{240}Pu → ^{34}Si + ^{206}Hg	91,323	24,25	26,97	26,25
^{241}Am → ^{34}Si + ^{207}Tl	94,218	25,30	28,80	28,44
^{240}Cm → ^{34}Si + ^{206}Pb	95,751	—	26,27	26,05

few iterations, and in the asymptotic region the iterative scheme rapidly converges to a solution. For n channels, the iterative procedure must usually be repeated n times in the entire region for each channel (and energy).

Initially we used in our estimates of the lifetime of cluster decay the simple potential (84), whose parameters were chosen from data on elastic scattering[71,72] or the cross section[73] of grazing collisions. The values of $\log T_c$ obtained with this potential are given in column 4 of Table V.

The calculated lifetimes are compared with the experimental times or with the predictions of experimental upper bounds (column 3). The theory and experiment agree to within 1–1.5 orders of magnitude.

It is interesting to estimate the effect of nuclear (quadrupole) deformation of the light fragment on the lifetimes or the deviation from spherical (diagonal) potentials used in Refs. 46 and 62. The results obtained with and without channel coupling (corresponding to deformed or spherical potentials) are represented in Fig. 19. As a rule, the corrections that arise from quadrupole distortions of the potential are important. First, these corrections depend on the fragment deformation. In the cases in which we studied cluster decay with the emission of fragments with large deformations,[74] such as ^{24}Ne ($\beta_2 = 0.41$) and ^{28}Mg ($\beta_2 = 0.48$), these corrections correspond to 0.5–1.5 orders of magnitude. An effect of the assumed coupling is an increase in the intensity of the cluster decay due to a lowering of each of the barriers in the initial family of barriers. We note that the "real" coupling was obtained by deformation of only the real nuclear potential.[73]

Comparing the results with and without allowance for the channel coupling, shown in Fig. 18, we can conclude that allowance for coupling decreases the lifetimes by a factor from 6 to 20. Nevertheless, the calculated value is still larger than the experimental value.

Lifetimes calculated with the same cluster-formation amplitudes[62] and Coulomb potential (84) but using the nuclear contact potential of Refs. 48 and 73 are shown in the upper part of Fig. 20. It can be seen that the calculated lifetimes for ^{24}Ne and ^{28}Mg emission are less than the experimental lifetimes, the difference between them being greater than the experimental errors (estimated at a few percent). As a rule, the lifetimes are shorter than in the preceding case, since the emission barriers are lowered by the influence of the large attractive nuclear potential. Therefore, the lifetimes will be shorter than the times T_c obtained with potentials that describe the scattering data.

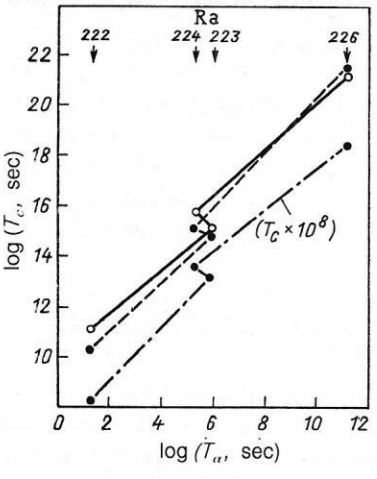

FIG. 19. The ($\log T_c$, $\log T_\alpha$) diagram for the isotopes ^{222,223,224,226}Ra: experimental data (continuous line) and the results of calculations[62] using shell (broken line) and resonance (chain line) formation amplitudes corresponding to the expressions (79) and (73).

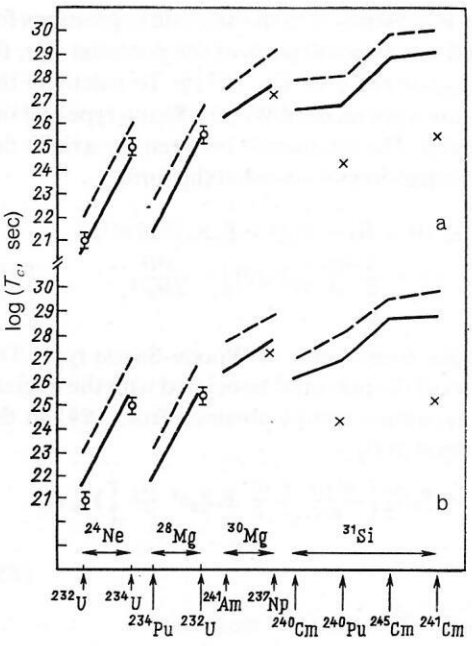

FIG. 20. Experimental lifetimes (open circles), experimental lower bounds (crosses), and calculated lifetimes with respect to spontaneous decay with emission of ^{24}Ne, $^{28-30}$Mg, and ^{34}Si clusters: the results of calculation with allowance for channel coupling (continuous lines) and without allowance (broken lines) are given for the potentials (84) (a) and (88) (b).

Nevertheless, the relatively small difference between these results with different nuclear potentials confirms the fact that the lifetimes depend weakly on the prescission uncertainty. In other words, large modifications of the nuclear potential at short distances between the fragments, when they overlap strongly, do not change the emission barriers which correspond to configurations with separate fragments, as was already noted in Ref. 47.

From analysis of the results in Fig. 18 it can be concluded that a spherical potential (obtained in the approximation of two spheres) tends to overestimate the barrier height, and also the lifetimes and half-lives. The differences between our results[70] obtained with and without allowance for channel coupling is large compared with the difference obtained in Ref. 47. This can be attributed to the large deformation length $\beta_L R_2$ used in Ref. 70 compared with the length $\beta_L R_2$ ($L = 1, 2, 3$) in Ref. 47.

In Fig. 18 it may be noted that for the emission of heavy fragments, such as ^{34}Si, the discrepancy between the theory and the experimental lower limits becomes appreciably greater.

Our results also agree with results known from processes that are the inverse of cluster-decay reactions, namely, below-barrier fusion of complex nuclei,[75,76] for which increases in the cross sections by up to two orders of magnitude are due to coupling to excited states.

As is well known, in the region Ra–U, where cluster

decay with emission of ^{14}C, ^{24}Ne, and ^{28}Mg was discovered, there were also found to be strong $E1$ transitions due to static octupole and dipole deformations.[88] There arises immediately the basic question of the connection between these deformations and the large cluster-formation amplitudes (and high intensities of cluster decay) in this region. This connection was studied in detail in Ref. 79. Besides the ground-state channel, the calculations also included channels corresponding to the excited 3^-, 5^-, and 2^+ levels in the ^{208}Pb nucleus in the reactions $^{223}Ra \rightarrow {}^{14}C + {}^{208}Pb$, $^{232}U \rightarrow {}^{24}Ne + {}^{208}Pb$, and $^{236}Pu \rightarrow {}^{28}Mg + {}^{208}Pb$. Matrix elements of the type (67) were calculated by means of the expressions (86) and (87). As a result, it was found that the influence of octupole deformations on T_c is 2–3 times less than in cases of quadrupole deformations (see Fig. 18). We note that our quantitative estimates are lower than the estimates obtained in Ref. 80 (only for ^{14}C emission from ^{223}Ra).

Effect of channel coupling

It was shown in Ref. 80 that the nondiagonal interaction (67) usually enhances cluster decay. In the traditional picture one determines the decay constant

$$\lambda = \lambda_0 F P_G, \tag{89}$$

where $\lambda_0 = (2Q/M_0)^{1/2} R_0$, and F is the formation factor.

In contrast to (14), the ground-state penetrability is

$$P_G = e^{\Delta_0} P^{(0)}(Q), \tag{90}$$

where

$$\Delta_0 = \sum_{i=1}^{N} (2/\hbar^2) \int_0^r dt\, V_i [r(t)]\, e^{-\omega_i t} \int_0^t dt'\, V_i [r(t')]\, e^{i\omega_i t'};$$

$$P^{(0)} = \exp\left[-\frac{2}{\hbar} \int_a^b dr\, [2M_0 (U(r) - Q)] \right]^{1/2};$$

$$r(0) = 0,\ V(r) = b,\ r(t) = a + \int_0^t dt' \left[\frac{2}{M_0} U(r) - Q \right]^{1/2},$$

in which V_i is the interaction that couples the excited mode with frequency ω_i, and $r(t)$ is the trajectory in the inverted potential. The coupling is determined in a macroscopic model:

$$V(r) = \frac{\beta R}{4\pi} \left[-\frac{\partial V_{\text{nuc}}}{\partial r} + \frac{3}{2} \frac{Z_1 Z_2 e^2}{2L+1} \frac{R^{L-1}}{r^{L+1}} \right], \tag{91}$$

where R is the nuclear radius, β is the deformation parameter of the mode (i), and L is the multipolarity.

In the actual calculations for ^{14}C emission from ^{223}Ra, allowance was made for the following channels associated with excitation of the 2^+, 3^-, 4^+, and 5^- states in ^{208}Pb with energies 4.1, 2.6, 4.3, and 3.2 MeV. For these parameters, we obtain

$$e^{\Delta_0} = 16; \tag{92}$$

$$P_G = 4{,}6 \cdot 10^{-25}. \tag{93}$$

Using in (89) the experimental value of λ, we can estimate

$$F(^{14}C) = 0{,}5 \cdot 10^{-8}; \tag{94}$$

$$F(^{14}C)/F(\alpha) \approx 10^7, \tag{95}$$

where $F(\alpha) \approx 0.04$ for ^{223}Ra.

The result (95) agrees excellently with the estimate of Ref. 2. We note that the nondiagonal interaction terms have the same form in Refs. 70 and 80.

Approximation of the spectroscopic factors

In Refs. 63 and 64, the decay constant is estimated on the basis of the formula

$$\lambda = \lambda_0 S \tag{96}$$

or

$$\Gamma = \Gamma_0 S, \tag{97}$$

where λ_0 is the single-particle decay constant, and S is the spectroscopic factor. The constant λ_0 is determined by the standard method (see Sec. 2): $\lambda_0 \approx (V/2R) P^{-1}$, where P is the barrier penetrability.

To calculate the spectroscopic factor S, we use shell wave functions in formulas of the type (79) and (80), and we take into account the effect of antisymmetrization in the cluster-formation amplitudes. The simple estimate[65]

$$S(A_2) \approx [S(\alpha)]^{(A_2-1)/3} \tag{98}$$

obviously overestimates $S(A_2)$, and integration (i.e., averaging) over the relative coordinates of the α particles and the pair of neutrons is not carried out.

A similar approximation was used in Ref. 64. It should be said that the results of Ref. 64 for the single-particle widths (see Table III) are always smaller than the results of Ref. 62 obtained with our formula (76) and also with the Breit formula (77). It is interesting that this difference increases with increasing cluster size. The difference arises in the first place from the different potentials which satisfy, in Ref. 62, and do not satisfy, in Ref. 64, the resonance condition at the decay energy.

We note that detailed calculations, especially for the emission of heavy clusters, have not yet been made in the framework of the microscopic approximation.[64]

In the treatments of Refs. 63 and 64, which are based on the R-matrix formalism and an integral (of Feshbach type) formalism, sufficient attention is not devoted to the important question of the boundary conditions that determine the formation of the unstable cluster states.

The complicated aspects of antisymmetrization of the cluster wave function (and, at the same time, cluster-formation amplitudes) were emphasized in both studies. Lack of space makes it impossible to discuss these questions here. For the clarification and understanding of these questions, we give some additional references to recent original studies (Refs. 81 and 82). In this direction, work is being done to improve the shell procedures for construction of the cluster-formation amplitudes.

Comparison of the results of microscopic semiempirical models with experiment

It is interesting to compare the results obtained in Refs. 61–63 and 65, in which, on the one hand, the shell model is used to describe the structure of the system, and on the other, it is assumed that the separated fragments move in a central potential with mass coefficient equal to the reduced mass of the two fragments. In comparing the results of these studies, one must bear in mind certain unimportant differ-

ences in the definition of the decay energy and the interaction potential. For example, in all studies the decay energy is calculated by means of the nuclear masses,[83] but only in Ref. 62 is allowance made for the effect of the screening of the electron shells on the decay energy. In these studies, two different parametrizations of the interaction potential are also used.[71,84]

Table VI gives the experimental values of T_c and the theoretical values predicted in Refs. 61–63 and 65.

As one can see in Table VI, the predicted lifetimes for spontaneous cluster decay agree with the experimental values, particularly for the light clusters (^{12}C and ^{24}Ne). The structure calculations are, when necessary, simplified in some respects, but they are evidently capable of reproducing the experimental data to an accuracy of 1–2 orders of magnitude.

The discrepancies of the ratios of the theoretical and experimental values are particularly large for the emission of ^{24}Ne from ^{232}U and ^{28}Mg from ^{234}U and ^{238}Pu. In this connection, we note that both of these clusters are strongly deformed,[74] and the approximation of a central interaction is not sufficiently accurate. Moreover, the discrepancies increase with increasing size of the emitted cluster, as was already noted in Refs. 61 and 62.

We note that the dependence of T_c on the mass, charge, and deformation of the emitted cluster was studied in detail in these investigations. The comparison of the results of the microscopic and macroscopic approaches made in Refs. 62 and 64 clearly shows that allowance for the nuclear structure leads to an increase in the lifetime of the radioactive nucleus. An analogous conclusion is known for α decay[89–92] and fission.[93–95] Without allowance for structure effects, heavy nuclei must decay rapidly. Thus the long lifetimes of heavy nuclei with respect to cluster decay are determined not only by the high Coulomb barriers but also by the nuclear-structure effects.

Finally, we note that, in contrast to the phenomenological models, particular attention is devoted in these studies to effects associated with allowance for the Pauli principle, pairing, the shell structure of nuclei, and dissipation of angular momentum. Allowance for these effects is a necessary condition for the creation of a consistent unified theory with good predictive power.

Enhancement of decay probability

Coupling to inelastic-excitation channels and few-nucleon transfer channels[70–80] does not exhaust the possibilities for enhancement of the probability of cluster decay. In Ref. 85 a mechanism of formation of a neck for fragments in contact was proposed as an enhancement mechanism. The coupling of the channels corresponding to the ground state of the fragments to channels in which a neck is formed causes a decrease of the potential energy (and the barrier) and, therefore, an increase of the decay rate.

In Refs. 62 and 64, one further possible mechanism for increasing the decay rate is discussed. It is assumed that the pairing of the nucleons, especially in heavy nuclei,[69] is very important, distinguishing the motion of pairs of nucleons with vanishing relative angular momentum and leading to the formation of a cluster having an α substructure. The coefficient of enhancement of the cluster decay is usually expressed in terms of the α-decay enhancement coefficient ($x_p, x_n \approx 10^3$).

In Ref. 86 it is assumed that in the region of overlap of the fragments (before separation) the pairing gap Δ_p becomes a dynamical parameter and that the potential energy and the mass parameter depend on this parameter [i.e., $V(r) \Rightarrow V(r,\Delta_p)$ and $M(r) \Rightarrow M(r,\Delta_p)$]. Estimates of the influence of this effect on the lifetimes of heavy nuclei with respect to cluster decay show that the enhancement coefficient (with "unfrozen" parameter Δ_p) is approximately equal to the coefficient obtained by coupling to the inelastic-excitation channels[80] ($K \sim 16$).

In Ref. 70, investigations were made of cluster decay with allowance for excitation of collective (rotational) levels of one fragment (see Sec. 5). We showed that because of the channel coupling the barrier for decay is reduced. This is evidently a further mechanism by which cluster decay can be enhanced.

Thus, the introduction of different degrees of freedom in addition to the relative distance leads to an increase in the

TABLE VI. Experimental and theoretical values of T_c. The theoretical values are obtained in the framework of the microscopic and semiempirical approaches.

Decay	log (T_c, sec)				
	Experiment	Theory (references in square brackets)			
		[61]	[62]	[63]	[65]
^{222}Ra (^{14}C)	11,02±0,06	11,7	10,5	11,8	11,2
^{223}Ra	15,2±0,05	15,2	14,9	15,1	15,3
^{224}Ra	15,9±0,12	16,4	15,3	16,2	16,1
^{226}Ra	21,33±0,2	18,24	21,7	21,1	21,2
^{230}Th (^{24}Ne)	24,64±0,09	22,6	26,4	24,8	24,4
^{231}Pa	23,38±0,08	19,85	23,9	23,4	21,6
^{232}U	21,06±0,1	22,5	19,8	20,8	20,2
^{233}U	24,82±0,15	24,5	24,4	25,4	23,7
^{234}U	25,25±0,05	24,6	28,0	25,6	25,5
^{234}U (^{26}Ne)	25,25±0,05	25,8	28,8	26,4	26,5
^{234}U (^{28}Mg)	25,75±0,06	23,8	25,7	25,4	25,7
^{238}Pu (^{28}Mg)	25,7±0,25	—	25,9	26,9	27,7
^{238}Pu (^{30}Mg)	25,9±0,75	22,9	28,5	25,8	25,6
^{238}Pu (^{32}Si)	25,3±0,16	—	27,7	25,7	26,0
^{241}Am (^{34}Si)	25,3	—	26,3	28,8	25,3

probability of cluster decay. A similar result was obtained for below-barrier fusion.[87]

CONCLUSIONS

In this review, the main attention has been devoted to phenomenological and microscopic approaches to the description of cluster decay. We have shown that they describe fairly well the average characteristics of cluster-decay processes, though the question of the actual decay mechanism still remains open. To solve this topical problem, we need additional experimental information on the emission of heavy clusters in the region of parent nuclei Pu–Fm, and also data that are the most sensitive to the mechanism of the process, for example, on the elementary excitation modes that transfer angular momentum and on the energies of the resonance states that can appear in complex systems. The relationship between cluster decay and triple fission must be studied in more detail.[88]

It would be of great interest to make a further phenomenological investigation of cluster decay on the basis of the most recent experimental data for the inverse processes (elastic and inelastic scattering, fusion).

In the majority of the phenomenological models of cluster decay, the parametrizations employed are not always adequate for these experimental data, and it is difficult to compare the corresponding theoretical and experimental parameters. Such a situation does not arise in the models of Refs. 61–65, 70, and 80, for which, as a rule, the parameters are completely determined by the parameters of the ion–ion potentials and the parameters of the forces between the different channels.

In the spirit of Refs. 62, 89, and 90, we have presented in detail an integral theory of cluster decay, in which, on the one hand, we make a microscopic (shell) calculation of the cluster-formation amplitude and, on the other, we take into account the influence of the interaction of the deformed fragments on the fragment-scattering process. The maximal decay probability is predicted fairly accurately on the basis of a study of the dependence of the cluster-formation amplitudes, the potential energy, and the decay energy Q on the shell effects and on the nuclear deformations.

For completeness of the dynamical treatment of cluster decay, we have also studied the case of resonance decay of a two-body system with a virtual level at an energy equal to the mean energy of the fragments. Comparing the results of the microscopic model and of the resonance (single-particle) approximation, we could estimate the total contribution of the structure effects to the lifetimes of the unstable nuclei and obtain reliable spectroscopic information.

Allowance for additional degrees of freedom (besides the relative distance) makes the theory more flexible for the description of the experimental data. However, this leads to an increase in the number of varied parameters, and to some extent this lowers the reliability of the predictions. It is obvious that as new experimental data become known on cluster decay from excited nuclei, and its relation to induced fission becomes clear, it will be possible to make a more detailed analysis of the phenomenon of cluster decay. It would, for example, be very valuable to know more about the properties of the phenomenon in the region of the nuclei Pu–Fm and also about the possibility of induced cluster decay (the analog of induced fission). In further investigations, one should study in detail the mechanism of formation and decay of nuclear quasimolecules. It is to be expected that accurate measurement of the resonance properties of the process will give information about the mechanism of the cluster-decay reaction.

Thus, we need further efforts on the part of the theoreticians and experimentalists in order to obtain a deeper understanding of the phenomenon of natural radioactivity.

There is now no doubt about the topical importance of the experimental problems of cluster decay listed above.

We should like to thank our colleagues R. Wunsch, Yu. S. Zamyatnin, L. P. Kaptar', I. N. Mikhaĭlov, V. V. Pashkevich, D. N. Poenaru, I. Rotter, V. G. Solov'ev, A. Săndulescu, and V. M. Shilov for their interest in the work, support, and discussion of the results.

[1] A. Săndulescu, D. N. Poenaru, and W. Greiner, Fiz. Elem. Chastits At. Yadra **11**, 1134 (1980) [Sov. J. Part. Nucl. **11**, 528 (1980)]; D. N. Poenaru and M. Ivascu, in *Proceedings of the Intern. School. J. Nucl. Phys. Poiana Brasov, 1980*, edited by A. Raduta, G. Stratan, and V. Zoran (Bucharest, 1981).
[2] J. H. Rose and G. A. Jones, Nature **307**, 245 (1984).
[3] D. V. Aleksandrov, A. F. Beliatski, Yu. A. Glukhov *et al.*, Pis'ma Zh. Eksp. Teor. Fiz. **40**, 152 (1984) [JETP Lett. **40**, 909 (1984)].
[4] S. Gales, E. Hourani, M. Hussonnois *et al.*, Phys. Rev. Lett. **53**, 759 (1984).
[5] W. Kutschera, I. Ahmad, and S. G. Amato, III, Phys. Rev. C **32**, 2036 (1985).
[6] P. B. Price, J. D. Stevenson, S. W. Barwic *et al.*, Phys. Rev. Lett. **54**, 297 (1985).
[7] S. W. Barwick, P. B. Price, H. L. Ravn *et al.*, Phys. Rev. C **34**, 362 (1986).
[8] F. Hourani, M. Hussonnois, L. Stab *et al.*, Phys. Lett. **160B**, 375 (1985).
[9] S. P. Tretyakova, A. Săndulescu, V. L. Micheev *et al.*, JINR Rapid Commun. **13**, 34 (1985).
[10] A. Săndulescu, Yu. S. Zamyatnin, I. A. Lebedev *et al.*, JINR Rapid Commun. **5**, 5 (1984).
[11] S. W. Barwick, P. B. Price, and J. D. Stevenson, Phys. Rev. C **31**, 1984 (1985).
[12] S. P. Tretyakova, A. Săndulescu, and Yu. S. Zamyatnin, JINR Rapid Commun. **7**, 23 (1985).
[13] S. W. Barwick, Ph.D. Thesis, University of California, Berkeley (1986).
[14] Shicheng Wang, P. B. Price, S. W. Barwick *et al.*, Phys. Rev. C **36**, 2717 (1987).
[15] K. J. Moody, E. K. Hulet, Shicheng Wang, and P. B. Price, Phys. Rev. C **39**, 2445 (1989).
[16] S. P. Tretyakova, Yu. S. Zamyatnin, V. N. Koventsev *et al.*, Preprint E7-88-803, JINR, Dubna (1988).
[17] Shicheng Wang, D. Snowden-Ifft, P. B. Price *et al.*, Phys. Rev. C **39**, 1647 (1989).
[18] K. J. Moody, E. K. Hulet, Shicheng Wang *et al.*, Phys. Rev. C **36**, 2710 (1987).
[19] M. Paul, I. Ahmad, V. Kutschera *et al.*, Phys. Rev. C **34**, 1980 (1986).
[20] P. B. Price, Ann. Rev. Nucl. Part. Sci. **39** (1989) (in press).
[21] D. N. Poenaru and M. Ivascu, J. Phys. (Paris) **45**, 1099 (1984).
[22] D. N. Poenaru and M. Ivascu, Rev. Roum. Phys. **29**, 623 (1984).
[23] D. N. Poenaru, M. Ivascu, A. Săndulescu, and W. Greiner, J. Phys. G **10**, L183 (1984).
[24] D. N. Poenaru, M. Ivascu, A. Săndulescu, and W. Greiner, Phys. Rev. C **32**, 572 (1985).
[25] D. N. Poenaru, M. Ivascu, A. Săndulescu, and W. Greiner, At. Data Nucl. Data Tables **34**, 423 (1986).
[26] G. Gamow, Z. Phys. **51**, 204 (1928); R. W. Gurney and E. U. Condon, Nature **122**, 429 (1928); H. A. Bethe, Rev. Mod. Phys. **9**, 161 (1937).
[27] N. Bohr and A. Wheeler, Phys. Rev. **56**, 426 (1939); J. Frenkel, Phys. Rev. **53**, 987 (1939).
[28] D. N. Trifonov, in *Radioactivity Yesterday, Today, and Tomorrow* [in Russian] (Atomizdat, Moscow, 1966), p. 38.
[29] Yu. A. Shukolyukov, in *Fission of Uranium Nuclei in Nature* [in Russian] (Atomizdat, Moscow, 1970), p. 240.
[30] E. Alexander, Science **172**, 821 (1971).
[31] V. V. Volkov, *Deep Inelastic Transfer Reactions* [in Russian] (Énergoatomizdat, Moscow, 1984).
[32] V. A. Karnaukhov and G. M. Ter-Akopyan, Phys. Rev. Lett. **12**, 339 (1965); V. I. Gol'danskiĭ, Usp. Fiz. Nauk **87**, 255 (1965) [Sov. Phys. Usp. **8**, 770 (1966)].
[33] H. Hofmann and K. Dietrich, Nucl. Phys. **A165**, 1 (1971).

[34] P. Ring, J. O. Rasmussen, and H. Massmann, Fiz. Elem. Chastits At. Yadra 7, 916 (1976) [Sov. J. Part. Nucl. 7, 366 (1976)].
[35] I. Perlman and J. O. Rasmussen, *Alpha Radioactivity, Handbuch der Physik*, Vol. 42 (Springer, Berlin, 1957), p. 109.
[36] M. Brack, J. Damgard, A. S. Jensen *et al.*, Rev. Mod. Phys. **44**, 320 (1972).
[37] I. Rotter, Fiz. Elem. Chastits At. Yadra **15**, 762 (1984) [Sov. J. Part. Nucl. **15**, 341 (1984)].
[38] W. D. Mayers and W. J. Swiatecki, Nucl. Phys. **81**, 1 (1966).
[39] E. H. J. Krappe and J. R. Mix, in *Proc. of the Symposium on Physics and Chemistry of Fission*, Vol. 1 (Vienna, 1974), p. 159.
[40] H. J. Krappe, R. J. Nix, and A. J. Sierk, Phys. Rev. C **20**, 992 (1979).
[41] D. N. Poenaru and M. Ivascu, *Lecture Notes In Physics* (Springer-Verlag, Berlin, 1987), p. 364.
[42] W. Greiner, M. Ivascu, D. N. Poenaru, and A. Săndulescu, in: *Treatise on Heavy Ion Science*, edited by D. A. Bromley (Plenum Press, New York, 1989), p. 116.
[43] D. N. Poenaru and M. Ivascu, in *Particle Emission from Nuclei, Vol. 2,* edited by D. N. Poenaru and M. Ivascu (CRC Press, Boca Raton, Florida, 1988), Chap. 8, p. 82.
[44] D. N. Poenaru, M. Ivascu, D. Mozilu *et al.*, Preprint IFIM-NP-66-68, Bucharest (1988).
[45] D. N. Poenaru and M. Ivascu, Prog. Theor. Phys. Suppl. (1989) (in press).
[46] Yi-Yan Shi and W. J. Swiatecki, Nucl. Phys. **A438**, 450 (1985).
[47] Yi-Yan Shi and W. J. Swiatecki, Nucl. Phys. **A464**, 205 (1987).
[48] G. A. Pik-Pichak, Yad. Fiz. **44**, 1421 (1986) [Sov. J. Nucl. Phys. **44**, 923 (1986)].
[49] P. B. Price, in: *Proc. of the Fifth Intern. Conf. on Nuclei Far from Stability, Rousseon Lake, Ontario, Canada*, edited by I. S. Towner (New York, 1988), p. 300.
[50] H. G. Carvalho, J. B. Martins, and O. A. P. Gavares, Phys. Rev. C **34**, 2261 (1986).
[51] M. Petrascu, A. Buta, and V. Simion, Preprint C.I.P. NP-44-1985, Bucharest (1985).
[52] M. Greiner and W. Scheid, J. Phys. G. **12**, L229 (1986).
[53] G. Shanmugan and B. Kamalaharam, Phys. Rev. C **38**, 1377 (1988).
[54] R. Herrmann, J. A. Maruhn, and W. Greiner, J. Phys. B **12**, L285 (1986).
[55] E. O. Fiset and J. R. Nix, Nucl. Phys. **A193**, 647 (1972).
[56] A. Sobiczewski, Fiz. Elem. Chastits At. Yadra **10**, 1170 (1979) [Sov. J. Part. Nucl. **10**, 466 (1979)].
[57] P. K. Gupta, Fiz. Elem. Chastits At. Yadra **8**, 717 (1977) [Sov. J. Part. Nucl. **8**, 289 (1977)].
[58] K. G. Thonas, Prog. Theor. Phys. **12**, 253 (1954).
[59] H. J. Mang, Z. Phys. **148**, 572 (1957).
[60] H. J. Mang, Ann. Rev. Nucl. Sci. **14**, 1 (1964).
[61] M. Iriondo, D. Jerrestam, and R. J. Liotta, Nucl. Phys. **A454**, 252 (1986).
[62] M. Ivascu and I. Silisteanu, Nucl. Phys. **A485**, 93 (1988).
[63] R. Blendowske and H. Walliser, Phys. Rev. Lett. **61**, 1930 (1988).
[64] S. G. Kadmenskiĭ, V. I. Furman, and Yu. M. Chuvil'skiĭ, in *Proc. of the International School on Nuclear Structure, Alushta, 14–22 October, 1985* [in Russian], p. 385.
[65] B. Buck and A. C. Merchant, Preprint No. 88/88, Oxford University (1988).
[66] A. Săndulescu, I. Silisteanu, and M. Rizea, Rev. Roum. Phys. **23**, 823 (1988); I. Silisteanu, Preprint E4-80-8, JINR, Dubna (1980).
[67] G. Breit, *Theory of Resonance Reactions and Allied Topics* (Springer-Verlag, Berlin, 1959).
[68] H. J. Mang and J. O. Rasmussen, K. Dan. Vidensk. Selsk. Mat.-Fys. Skr. **3**, 1 (1962).
[69] V. G. Soloviev, *Theory of Complex Nuclei* (Pergamon Press, Oxford, 1976) [Russ. original, later ed., Énergoatomizdat, Moscow, 1982].
[70] I. Silisteanu and M. Ivascu, Preprint CIP-Bucharest FT-335 (1988); J. Phys. G. **15**, 1405 (1989).
[71] R. P. Cristiansen and W. Winter, Phys. Lett. **65B**, 19 (1977).
[72] J. J. Kolota, K. E. Rehm, D. C. Kovar *et al.*, Phys. Rev. C **30**, 125 (1984).
[73] E. E. Gross, T. P. Cleary, J. L. C. Ford *et al.*, Phys. Rev. C **29**, 459 (1984).
[74] S. M. Ramau, C. H. Malarkey, and W. T. Milner, At. Data Nucl. Data Tables **36**, 1 (1987).
[75] A. V. Tarakanov and V. M. Shilov, Yad. Fiz. **48**, 109 (1988) [Sov. J. Nucl. Phys. **48**, 68 (1988)].
[76] T. Udagawa, B. T. Kim, and T. Tamura, Phys. Rev. C **32**, 124 (1985).
[77] B. B. Beck, T. P. Betts, J. E. Gindler *et al.*, Phys. Rev. C **33**, 195 (1985)
[78] A. J. Baltz and B. F. Baymah, Phys. Rev. C **26**, 1969 (1982).
[79] I. Silisteanu and M. Ivascu, Preprint CIP-TP-46, Bucharest (1989).
[80] S. Landowne and C. H. Dasso, Phys. Rev. C **33**, 387 (1986).
[81] A. Florescu, S. Holan, and A. Săndulescu, Rev. Roum. Phys. **33**, 131 (1988).
[82] A. Florescu, S. Holan, and A. Săndulescu, Rev. Roum. Phys. **33**, 243 (1988),
[83] A. H. Wapstra and G. Audi, Nucl. Phys. **A432**, 1 (1985).
[84] B. Buck, C. B. Dower, and J. P. Vary, Phys. Rev. C **11**, 1803 (1975).
[85] F. Barranco, R. A. Broglia, and G. F. Bertsch, Phys. Rev. Lett. **60**, 507 (1988).
[86] A. Săndulescu, J. Phys. G. **15**, 529 (1989).
[87] V. P. Permyakov and V. M. Shilov, Fiz. Elem. Chastits At. Yadra **20**, 1396 (1989) [Sov. J. Part. Nucl. **20**, 594 (1989)].
[88] P. Schall, P. Heeg, M. Mutterer *et al.*, Phys. Lett. **191B**, 339 (1988).
[89] A. Săndulescu, I. Silisteanu, and R. Wunsch, Nucl. Phys. **A305**, 205 (1970).
[90] R. G. Nazmitdinov and I. Silisteanu, Yad. Fiz. **43**, 58 (1986) [Sov. J. Nucl. Phys. **43**, 36 (1986)].
[91] O. Dumitrescu, Fiz. Elem. Chastits At. Yadra **10**, 377 (1979) [Sov. J. Part. Nucl. **10**, 147 (1979)].
[92] S. G. Kadmenskiĭ and V. I. Furman, Fiz. Elem. Chastits At. Yadra **6**, 469 (1975) [Sov. J. Part. Nucl. **6**, 189 (1975)].
[93] V. V. Pashkevich, Nucl. Phys. **A477**, 1 (1988).
[94] Z. Patik, A. Sobiczewski, P. Ambruster *et al.*, Nucl. Phys. **A491**, 267 (1989).
[95] S. Cwiok, P. Rozmej, A. Sobiczewski *et al.*, Nucl. Phys. **A491**, 281 (1989).
[96] C. M. Lederer and V. S. Shirley, *Tables of Isotopes* (Wiley, New York, 1978).
[97] M. Razavy and A. Pinepole, Phys. Rep. **168**, 305 (1988).

Translated by Julian B. Barbour